Investigation on Syntheses of Nanocolloids and Their Thermophysical Properties

Thèse présentée à la Faculté des Sciences
Institut de Physique
Université de Neuchâtel

Par

Natallia Shalkevich

Acceptée sur proposition du jury :

Prof. T. Bürgi, directeur de thèse
Prof. H. Stöckli-Evans, rapporteur
Prof. G. Süss-Fink, rapporteur
Prof. F. Scheffold, rapporteur

Soutenue le 22 septembre 2009

Université de Neuchâtel
2009

Université de Neuchâtel

FACULTE DES SCIENCES
Secrétariat-Décanat de la faculté
- Rue Emile-Argand 11
- CP 158
- CH-2009 Neuchâtel

IMPRIMATUR POUR LA THESE

Investigation on syntheses of Nanocolloids and their thermophysical properties

Natallia SHALKEVICH

UNIVERSITE DE NEUCHATEL

FACULTE DES SCIENCES

La Faculté des sciences de l'Université de Neuchâtel,
sur le rapport des membres du jury

Mme H. Stoeckli-Evans (co-directrice de thèse),
MM. T. Bürgi (co-directeur de thèse, Heidelberg D),
G. Süss-Fink et F. Scheffold (Fribourg)

autorise l'impression de la présente thèse.

Neuchâtel, le 24 septembre 2009

Le doyen :
F. Kessler

UNIVERSITE DE NEUCHATEL
FACULTE DES SCIENCES
Secrétariat - décanat de la faculté
Rue Emile-Argand 11 - CP 158
CH-2009 Neuchâtel
felix Kessler

Abstract

This thesis explores the thermophysical properties of nanocolloids. We focus here on preparation and thermal conductivity measurements of various colloidal systems consisting of different gold and ceramic particles, which are studied both in their natural state as well as chemically (surface) modified. The colloidal suspensions of nanoparticles (so-called nanofluids) have recently attracted particular attention in applied research as fluids with advanced thermal conductivity combined with good transport properties.

To enhance the properties of nanofluids, it is crucial to obtain high concentrations of the solid particles. The direct synthesis of stable, highly concentrated colloids is also very important for more complex studies. We demonstrate a new way for the preparation of nearly mono-dispersed stable gold colloids with a fairly high concentration using a two step procedure. First we synthesize citrate capped gold nanoparticles and then exchange the citrate ions by triethyleneglycolmono-11-mercaptoundecylether (EGMUDE). This leads to the immediate precipitation and formation of composite assemblies. The prepared gold colloid can be easily concentrated up to 20 times by separation of the flocculated part. Moreover, we show that the gold nanoparticles were successfully self-redispersed after few days and stay stable at high concentrations over months. UV–visible spectra, transmission electron microscopy (TEM), and dynamic light scattering (DLS) are used to characterize the products thus formed and a new model of surfactant composite assembly formation is proposed.

As a model system to evaluate the effect of the particle size, concentration, stabilization method and particle clustering on the thermal conductivity, we use gold nanofluids. We synthesized spherical gold nanoparticles of different size (from 2 nm to 45 nm) and prepared stable gold colloids in the range of volume fraction of 0.00025–1 %. The particles are either protected solely by citrate ions or covered by chemically bound ionic or nonionic stabilizers. We investigate the influence of these parameters as well as the temperature on the thermal conductivity of gold nanofluids

by both steady state parallel plate (GAP) and transient hot-wire (THW) methods. Obtained thermal conductivity data are consistent with effective medium theory.

In order to test the effect of dispersed materials, different kinds of commercial ceramic nanoparticles (AlN, Al_2O_3, $MgO*Al_2O_3$, ZnO, CuO, TiO_2, SiO_2, $SiO_2*Al_2O_3$) suspended in water were investigated. Thermal conductivity of nanofluids was measured by the transient hot wire technique. The effects of particle volume fraction, particle shape and dispersal agent were studied. Different models of heat transfer in nanofluids were applied in order to estimate the thermal conductivity of ceramics suspensions and to compare with experimental data.

Finally, we investigate the thermal conductivity of concentrated colloids in fluid, glass and gel states at equal volume fractions. We use two kinds of nanoparticles (SiO_2 and Al_2O_3) with significantly different thermal conductivity in the solid state. Thermal conductivity of the three states was measured as a function of volume fraction. Different local dynamical properties of the particles allow us to gain insight on various mechanisms of heat transfer in nanofluids. While in fluid (nanofluid) and gel (interconnected particles) states we observed expected enhancement of thermal conductivity, glassy samples (isolated frozen particles) exhibit a significant decrease of the thermal conductivity compared to the base fluid. Obtained data are analyzed in terms of existing models and possible explanations of the thermophysical properties of different colloidal states are proposed.

Abbreviations

B

BYK	ammonium salt of an acrylate polymer

C

CMC	critical micelle concentration
CTAB	cetyltrimethylammonium bromide

D

DLS	dynamic light scattering

E

EDL	electrical double layer
EGMUDE	triethyleneglycolmono-11-mercaptoundecylether
EGUDE	triethyleneglycolundecylether

G

GSH	L-glutathione reduced

N

NAC	N-acetyl-L-cysteine

S

SPR	surface plasmon resonance

T

TEM	transmission electron microscopy
THW	transient hot-wire method
TMeAOH	tetramethylammonium hydroxide

Table of contents

Key words

Gold, ceramic nanoparticles, concentrated nanocolloids, nanofluids, composite assemblies, gel, glass
Synthesis, surface modification, stabilization
Thermal conductivity, heat transfer
Transmission electron microscopy, UV-visible spectroscopy, dynamic light scattering method, transient hot-wire method, steady state parallel plate method

Mots clés

Or, nanoparticules céramiques, nanocolloïdes concentrés, nanofluides, assemblages composites, gel, verre
Synthèse, modification de surface, stabilisation
Conductibilité thermique, transfert de chaleur
Microscopie électronique en transmission, spectroscopie UV-visible, méthode de diffusion dynamique de la lumière, méthode du fil chaud en régime transitoire, méthode des plaques parallèles en régime permanent

Introduction

Introduction

A colloid is a system consisting of at least two separate phases i.e. a dispersed phase (internal phase) and a continuous phase (dispersion medium). The dimension of dispersed phase has traditionally been considered to be in the submicroscopic range but greater than the atomic size region that is within the range from 1 nm to 1 μm. In this work we operate with the term «nanocolloid» to underline the nanometer size of dispersed phase (nanoparticles) from 1 nm to 100 nm. The colloidal system has two peculiarities i.e. a dispersity (the presence of the phase which is dispersed into another) and a heterogeneity (the presence of interfaces between the components of the colloid). They result in molecular-kinetic properties of colloids such as Brownian motion (thermal motion) of suspended particles, their osmosis, diffusion, sedimentation, on the one hand, and, on the other hand, exhibit peculiar to the bulk system properties. This endows the nanocolloids with originality and makes the nanocolloids attractive for different research and industrial domains. Because the nanocolloids occupy the intermediate place between single elements (atoms) and bulk structures there are two main ways of their production, which are illustrated in Figure 1.

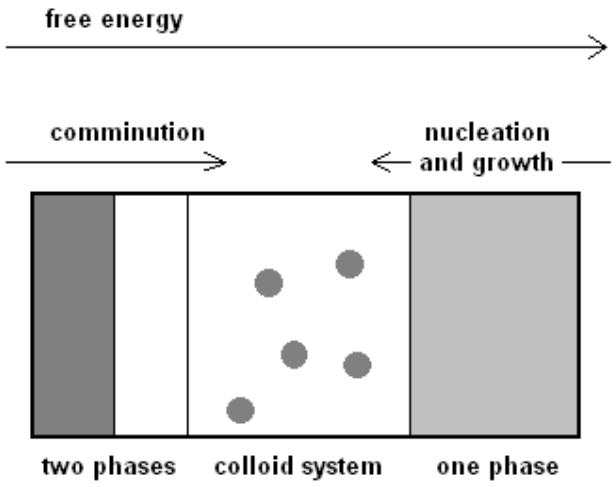

Figure A. Principle ways to prepare colloids.

Comminution is a mechanical process of dispersing of bulk phase in the grained phase that results in increase of interface area. Mechanical abrasion and ultrasonic radiation are examples of the comminution process. Preparation of colloidal system by this method requires mechanical work that often is accompanied by large energy consumption. Furthermore the resulting colloids are polydisperse systems with wide size distribution of dispersed phase. Another means of producing nanomaterials is the so-called condensation method including two processes such as nucleation and growth. Nucleation is a first step of phase transformation when an aggregation of atoms (nuclei) is formed. The growth of nuclei is a second step which results in the formation of large crystalline particles. Nucleation and growth occur with a decrease in free energy, through a change in some thermodynamic parameters (temperature, pressure, concentration, including addition of new component). This method is better controlled than comminution and better tuning of the particle size distribution can be achieved by manipulating the state of super-saturation of the nucleating species and by addition of surfactants to protect the incipient dispersed particles against coagulation or coalescence that can take place during the nuclei growth. Accumulation of free energy (surface free energy) during a new phase (nanoparticles) formation can cause an irreversible agglomeration of colloid particles. The latter can be suppressed through an additional stabilization of a well-developed interface by a surface charge or/and protective surface layer of modifier (sterical stabilization). Highly stable colloids are widely used as catalysts, pigments, drug carriers etc. Quite recently nanocolloids were also proposed as heat transfer agent. In this case high thermal conductivity of the dispersed phase is combined with good transport properties of the dispersive fluid.

Thermal conductivity (λ) is the intrinsic property of a material, which relates to its ability to conduct heat. It can be thought of as a flux of heat ($\partial Q/(A*\partial t)$) divided by a temperature gradient ($\partial T/x$):

$$\lambda = \frac{\partial Q \cdot x}{A \cdot \partial t \cdot \partial T}$$

where Q = the heat,

A = the total cross section area of conducting surface,

t = the time,

x = the thickness of surface separating the two phases at different temperatures T.

Heat is normally conducted by the transfer of energy of motion between neighbouring molecules in a liquid, gas or solid. In a gas, energy transfers through molecular collisions. In metallic solids, an additional mechanism of energy transfer via “free electrons” is also important. While heat transfer by conduction involves transfer of energy within a material without any motion of the material as a whole the total heat transfer also included two other modes: convection and radiation. In convection, heat is transferred by bulk transport and mixing of macroscopic fluid (volume) elements. Recall that there can be forced convection, where the fluid is forced to flow via mechanical means, or natural convection, where density differences cause fluid elements to flow. Radiation differs from conduction and convection in that no medium is needed for its propagation. Radiation is the transfer of energy through space by means of electromagnetic waves.

Thermal conductivity of the liquids is mainly determined by their viscosity and heat capacity. Nevertheless, convection is also an important contribution to the overall heat transfer. For a solid material such as an elemental metal, the link between thermal conductivity and viscosity loses its validity and only the connection with heat capacity is still valid. Thermal conductivity of the solids and its temperature dependence is strongly depends on the nature of the heat carrier. Heat can be transferred either by electrons or phonons or their combination. The ratio of mean free paths of the electrons and phonons determines temperature dependence of the thermal conductivity. Thus, highly ordered materials such as pure metals, most pure ceramics, and crystalline polymers exhibit increasing thermal conductivity with decreasing temperature due to increases in both the electronic and phonon mean free paths at low temperatures. On the other hand the disordered materials such as solid–solution alloys, inorganic glasses and glassy polymers, exhibit decreasing thermal conductivity with decreasing temperature. This is because the electronic and phonon mean free

paths are relatively small at all temperatures, and temperature variation in heat capacity dominates the temperature dependence of thermal conductivity. The situation becomes even more complex in case of heterogeneous, multiphase systems. To a first approximation, the thermal conductivity in these systems can be approximated through heat capacity by a weighted average of the component heat capacities. Nevertheless, the thermal conductivity of heterogeneous systems is impossible to predict on heat capacity alone.

The colloidal suspensions of solid nanoparticles called nanofluids have recently attracted great interest as new-generation of heat transfer fluids. They are expected to have superior properties compared to conventional heat transfer fluids, as well as fluids containing micro-sized solid particles. A large number of experimental studies of nanofluids with different kinds of dispersed solid phases have been reported. Research has shown that relatively small loading of nanoparticles, of the order of 5 volume per cent or less, can increase thermal conductivity of the base fluid to a large extent. Extreme results were obtained for different allotropes of carbon. Thus, enormous enhancements of thermal conductivity by 160% and by 70% were observed for a suspension containing 1% of MWCNTs in oil[1] and for 1% ultra-dispersed diamond in ethylene glycol respectively.[2] Various types of nanoparticles such as metallic[3-7] and non-metallic[1, 2, 8-12] were investigated. Peng Hu at al.[12] demonstrated a 20% increase in thermal conductivity of ethanol with addition of 4 vol% of AlN particles with diameter of 20 nm. The 1 vol% suspensions of 35 nm CuO in ethylene glycol and of 7 nm SiO_2 in water have shown 9 % and 3 % enhancement of thermal conductivity respectively.[9] It is interesting to note, that some aqueous nanofluids at vanishing concentrations of “naked” metallic particles such as 50-100 nm copper at 0.001 volume fraction[4] and 10-20 nm gold at 0.00026 vol%[5] were reported to yield thermal conductivity enhancements by up to 23.8% and 21% (at 60 °C) respectively.

The thermal conductivity of solid-liquid mixtures of relatively large particles (micro-sized) at low solid concentration can be predicted within classical Maxwell model.[13] This model determines the effective thermal conductivity from the thermal conductivities of the base fluid and the solid particles and the volume fraction of the solid phase and is given by

$$\frac{\lambda_e}{\lambda_0} = \frac{\lambda_p + 2\lambda_0 + 2(\lambda_p - \lambda_0)\varphi}{\lambda_p + 2\lambda_0 - (\lambda_p - \lambda_0)\varphi},$$

where λ_e = the effective thermal conductivity of the nanofluid,

λ_0 = the thermal conductivity of the base fluid,

λ_p = the thermal conductivity of the particles,

φ = the volume fraction of the particles.

Many later proposed models have been based on the Maxwell model. Thus, the Bruggeman model[14] is applied to spherical particles with no limitation on the concentration of components and the Hamilton-Crosser model[15] introduces a shape factor to account for the effect of the shape of the particles. The revised Maxwell model, proposed by Yu and Choi,[16] includes the effect of interfacial layer thickness but is validated with very limited experimental data and only applies under certain conditions.

The classical models include only the particle shape and particle volume fraction as variables and assume diffusive heat transfer in both liquid and solid phases and do not consider additional mechanisms of heat transfer in nanofluids. Therefore in many cases, they are unable to accurately predict the thermal conductivity of nanofluids. Several mechanisms have been recently proposed to account for the thermal conductivity of nanofluids beyond the Maxwell prediction. These include Brownian motion[17, 18] of the nanoparticles, fluid convection at the micro scale,[19, 20] liquid layering at the particle-fluid interface,[11, 16, 21, 22] clustering of the nanoparticles[2, 23-25] or a combination of aforementioned mechanisms.[26, 27]

Main goal of this study is the preparation of high performance nanofluids that can be used for cooling of microelectronic devices. As a starting point we considered some recent publications that claimed unusually high increase of thermal conductivity for very diluted gold nanocolloids. The influence of several parameters on thermal properties of the nanofluid should be considered. This implies the preparation of stable and concentrated aqueous gold nanocolloids in a wide particle size range. Afterwards we should study the influence of particle size, particle concentration,

particle material (metallic, ceramic) and the nature of the stabilizer on the thermal conductivity of nanofluids. Finally, we should shed the light on the mechanism of heat transfer in such nanocolloids by studying the thermophysical properties of SiO_2 and Al_2O_3 nanocolloids in fluid, gel, glass states.

References

1. Choi, S. U. S.; Zhang, Z. G.; Yu, W.; Lockwood, F. E.; Grulke, E. A., Anomalous thermal conductivity enhancement in nanotube suspensions. *Applied Physics Letters* **2001,** 79, (14), 2252-2254.
2. Kang, H. U.; Kim, S. H.; Oh, J. M., Estimation of Thermal Conductivity of Nanofluid Using Experimental Effective Particle Volume. *Experimental Heat Transfer* **2006,** 19, (3), 181 - 191.
3. Putnam, S. A.; Cahill, D. G.; Braun, P. V.; Ge, Z.; Shimmin, R. G., Thermal conductivity of nanoparticle suspensions. *Journal of Applied Physics* **2006,** 99, (8), 084308.
4. Liu, M.-S. L., Mark Ching-Cheng; Tsai, C.Y. ; Wang, C.-C., Enhancement of thermal conductivity with Cu for nanofluids using chemical reduction method. *International Journal of Heat and Mass Transfer* **2006,** 49, (17-18).
5. Patel, H. E.; Das, S. K.; Sundararajan, T.; Nair, A. S.; George, B.; Pradeep, T., Thermal conductivities of naked and monolayer protected metal nanoparticle based nanofluids: Manifestation of anomalous enhancement and chemical effects. *Applied Physics Letters* **2003,** 83, (14), 2931-2933.
6. Hong, T.-K.; Yang, H.-S.; Choi, C. J., Study of the enhanced thermal conductivity of Fe nanofluids. *Journal of Applied Physics* **2005,** 97, (6), 064311-4.
7. Assael, M.; Metaxa, I.; Kakosimos, K.; Constantinou, D., Thermal Conductivity of Nanofluids – Experimental and Theoretical. *International Journal of Thermophysics* **2006,** 27, (4), 999-1017.
8. Li, C. H.; Peterson, G. P., Experimental investigation of temperature and volume fraction variations on the effective thermal conductivity of

nanoparticle suspensions (nanofluids). *Journal of Applied Physics* **2006,** 99, (8), 084314.

9. Hwang, Y. J.; Ahn, Y. C.; Shin, H. S.; Lee, C. G.; Kim, G. T.; Park, H. S.; Lee, J. K., Investigation on characteristics of thermal conductivity enhancement of nanofluids *Current Applied Physics* **2006,** 6, (6), 1068.
10. Zhu, H. T.; Zhang, C. Y.; Tang, Y. M.; Wang, J. X., Novel Synthesis and Thermal Conductivity of CuO Nanofluid. *The Journal of Physical Chemistry C* **2007,** 111, (4), 1646-1650.
11. Lee, D., Thermophysical Properties of Interfacial Layer in Nanofluids. *Langmuir* **2007,** 23, (11), 6011-6018.
12. Hu, P.; Shan, W.-L.; Yu, F.; Chen, Z.-S., Thermal Conductivity of AlN–Ethanol Nanofluids. *International Journal of Thermophysics* **2008,** 29, (6), 1968-1973.
13. Maxwell, J. C., *Electricity and magnetizm*. Clarendon Press: Oxford, 1873.
14. Bruggeman, D. A. G., Berechnung verschiedener physikalischer Konstanten von heterogenen Substanzen. I. Dielektrizitдtskonstanten und Leitfдhigkeiten der Mischkцrper aus isotropen Substanzen. *Annalen der Physik* **1935,** 416, (7), 636-664.
15. Hamilton, R.; Crosser, O. K., Thermal conductivity of heterogeneous two-component systems. *Industrial and Engineering Chemistry Fundamentals* **1962,** 1, (3), 187-191.
16. Yu, W.; Choi, S. U. S., The Role of Interfacial Layers in the Enhanced Thermal Conductivity of Nanofluids: A Renovated Maxwell Model. *Journal of Nanoparticle Research* **2003,** 5, (1), 167-171.
17. Kumar, D. H.; Patel, H. E.; Kumar, V. R. R.; Sundararajan, T.; Pradeep, T.; Das, S. K., Model for Heat Conduction in Nanofluids. *Physical Review Letters* **2004,** 93, (14), 144301.
18. Bhattacharya, P.; Saha, S. K.; Yadav, A.; Phelan, P. E.; Prasher, R. S., Brownian dynamics simulation to determine the effective thermal conductivity of nanofluids. *Journal of Applied Physics* **2004,** 95, (11), 6492-6494.
19. Jang, S. P.; Choi, S. U. S., Role of Brownian motion in the enhanced thermal conductivity of nanofluids. *Applied Physics Letters* **2004,** 84, (21), 4316-4318.

20. Prasher, R.; Bhattacharya, P.; Phelan, P. E., Thermal conductivity of nanoscale colloidal solutions (nanofluids). *Physical Review Letters* **2005,** 94, (2), 025901.

21. Keblinski, P.; Phillpot, S.; Choi, S.; Eastman, J., Mechanisms of heat flow in suspensions of nano-sized particles (nanofluids). *International Journal of Heat and Mass Transfer* **2002,** 45, 855-863.

22. Leong, K. C.; Yang, C.; Murshed, S. M. S., A model for the thermal conductivity of nanofluids – the effect of interfacial layer. *Journal of Nanoparticle Research* **2006,** 8, (2), 245-254.

23. Prasher, R.; Evans, W.; Meakin, P.; Fish, J.; Phelan, P.; Keblinski, P., Effect of aggregation on thermal conduction in colloidal nanofluids. *Applied Physics Letters* **2006,** 89, (14), 143119.

24. Prasher, R.; Phelan, P. E.; Bhattacharya, P., Effect of Aggregation Kinetics on the Thermal Conductivity of Nanoscale Colloidal Solutions (Nanofluid). *Nano Letters* **2006,** 6, (7), 1529-1534.

25. Philip, J.; Shima, P. D.; Raj, B., Nanofluid with tunable thermal properties. *Applied Physics Letters* **2008,** 92, (4), 043108.

26. Wang, B.-X.; Zhou, L.-P.; Peng, X.-F., A fractal model for predicting the effective thermal conductivity of liquid with suspension of nanoparticles *International Journal of Heat and Mass Transfer* **2003,** 46, (14), 2665-2672.

27. Xuan, Y.; Li, Q.; Hu, W., Aggregation structure and thermal conductivity of nanofluids. *AIChE Journal* **2004,** 49, (4), 1038-1043.

Chapter 1

Reversible formation of gold nanoparticle – surfactant composite assemblies for the preparation of concentrated colloidal solutions

Reversible formation of gold nanoparticle – surfactant composite assemblies for the preparation of concentrated colloidal solutions

Authors: Natallia Shalkevich, Andrey Shalkevich, Lynda Si-Ahmed and Thomas Bürgi

1.1 Abstract

We have developed a simple method for the preparation of nearly mono-dispersed stable gold colloids with a fairly high concentration using a two step procedure. First we synthesize citrate capped gold nanoparticles and then exchange the citrate ions by triethyleneglycolmono-11-mercaptoundecylether (EGMUDE). This leads to the immediate precipitation and formation of composite assemblies. The gold nanoparticles were successfully self-redispersed after few days. The prepared gold colloid can be easily concentrated up to 20 times by separation of the flocculated part. UV–visible spectra, transmission electron microscopy (TEM), and dynamic light scattering (DLS) were used to characterize the products thus formed.

Keywords: gold colloid, dynamic light scattering, agglomeration, stabilization

1.2 Introduction

During the past years, the synthesis and characterization of nanoparticles has become the focus of both fundamental science and technical applications because of their unique characteristics such as catalytic activity, optical, electronic, thermal, magnetic [1] and other properties[2]. In particular, gold nanoparticles are currently being explored for example in catalysis[3], chemical sensing[4, 5], molecular labeling[6], gene delivery[7], and photonics[7].

There are many established methods for gold colloid syntheses, such as conventional chemical reduction[8], heat-treatment[9], microwave irradiation[10, 11], sonochemical[12], photolytical[13] and seeding growth approach[14], to mention a few. Most of those methods utilize thiols as capping agents in order to improve nanoparticle stability. Thiolated modifiers provide enhanced stabilization through the sterical interaction between surface layers and/or their charge repulsion. Nevertheless only relatively dilute colloids can be obtained by direct reduction because concentrated solutions result in the formation of a precipitate. Another problem arises from the fact that larger gold nanoparticles (above 15-20 nm) require significantly stronger stabilization to prevent agglomeration.

In this paper, we report the facile synthesis of gold nanoparticles by using the Turkevich, Frens[15] method with further ligand exchange. We have made the discovery that triethyleneglycolmono-11-mercaptoundecylether (EGMUDE) in the presence of citrate capped gold in an aqueous medium is able not only to yield highly stable nanoparticles but also segregates them into a concentrated phase. In contrast to previous syntheses where the prepared colloid needs to be additionally concentrated, the current synthesis provides suspensions of highly stable gold nanoparticles at high concentration.

1.3 Experimental section

1.3.1 Materials

Hydrogen tetrachloroaurate (III) solution was supplied by Metalor Technologies SA, Neuchâtel, Switzerland. Trisodiumcitrate dihydrate and triethyleneglycolmono-11-mercaptoundecylether (95%) (EGMUDE) were purchased from Sigma-Aldrich. Ethanol (99.9%) was purchased from Merck. All reagents were used as received. Milli-Q (Millipore) water with a resistivity of 18.2 MΩ was employed throughout. Dialysis membranes (3.5 kDa, Spectra/Por CE) were obtained from Spectrum.

1.3.2 Instrumentation

UV-visible spectra (200-900 nm) were recorded on a Cary 300 spectrometer using a quartz cell of 1 cm path length. Transmission electron micrographs (TEM) were obtained with a Philips C 200 microscope in bright field mode at a voltage of 200 kV. The samples for TEM study were prepared by casting a few drops of the gold colloid onto carbon-coated copper grids (300 mesh) and used after solvent evaporation in air.

Dynamic light scattering (DLS) was performed with an ALV-5000 spectrophotometer equipped with an argon-laser (Coherent, model Innova 300, λ = 488 nm), a digital autocorrelator (ALV) and variable angle detection system. Measurements were made at a fixed scattering angle of 90° and a temperature of 25.0 ± 0.1 °C. The individual correlation functions were analyzed using a second-order cumulant fit.

1.3.3 Synthesis of gold nanoparticles

17 nm gold nanoparticles were prepared by the classical method described by Turkevich and Frens[15, 16]. 50 ml of Milli-Q water slightly stirring was heated to 90° C in a flat-bottomed flask closed by a cover-glass. 6.5 µl of hydrogen tetrachloroaurate (III) solution (0.028 mmol) was quickly added into hot water and then heated to 97-98°C. 24.9 mg of sodium citrate (0.084 mmol) was dissolved in 1.25 ml of Milli-Q water and rapidly introduced into the boiling gold solution. A color change from pale

yellow over colourless to red-wine took place in 15 s. The mixture was kept boiling for 15 min and then cooled to room temperature.

1.3.4 Preparation of EGMUDE modified gold nanoparticles

Gold colloid was purified via dialysis before ligand addition. For this, 50 ml of gold-citrate colloid was transferred to a 3.5 kDa membrane and dialyzed against Milli-Q water in a 2L beaker. The water was changed every 10 h in the course of a week. After dialysis not more than 10% of the gold was lost, as was determined by UV-vis spectroscopy from the absorption of the plasmon band.

Functionalization of the gold nanoparticles with EGMUDE was accomplished by ligand addition to dialyzed citrate stabilized gold colloid in a 1:2.5 molar ratio of Au atoms to thiol molecules. EGMUDE was added as a colloidal solution (micellar solution), which was prepared in the following way: 0.07 mmol of thiol was added to 5 ml of Milli-Q water and stirred for 2 min. The emulsion was injected into 50 ml of well stirred gold colloid (initial gold concentration of 0.55 mM was diminished to 0.5 mM after dialysis). The color of the mixture quickly turned to black, the particles seemed to agglomerate. Without the stirring the particles were precipitated at the bottom of the flask. After one day, if to shake the slightly colored sediment, the particles were back into solution indicating that the agglomeration process was reversible. After 5 days, the particles were completely redispersed without any need to stir them.

The water was rotary evaporated and EGMUDE-modified gold particles were washed with a small quantity of ethanol to remove the excess thiol. This purification method relies on the fact that the free thiol is soluble in ethanol, whereas the particles are hardly soluble. The gold nanoparticles were re-dispersed in a small volume of water, up to a concentration of 1 vol%. Under these conditions the particles could be kept at least for several months without noticeable change.

Use of the gold colloid without dialysis for the modification with EGMUDE was not successfull. In fact, the thiol exchange took place but no formation of supramolecular agglomerates was observed. The effect of the dialysis is a reduction of

the ion strength (citrate and sodium ions), which leads to an increase of the width of the electrical double layer. The gold-EGMUDE nanoparticles formed without the dialysis (in the absence of supramolecular assemblies) were less stable than the ones formed within the assemblies, i.e. with the dialyzed sample, which indicates uncomplete ligand exchange. In fact, during the cleaning with ethanol a part of the particles prepared with the undialyzed gold colloid showed irreversible agglomeration, whereas the sample prepared within the supramolecular assemblies was perfectly stable.

1.4 Results and discussion

Citrate stabilized gold colloid

The thermal citrate reduction of gold(III) in a 1:3 Au:citrate molar ratio produced homogeneous spherical particles with a diameter of ca. 17 nm (Figure 1.1a).

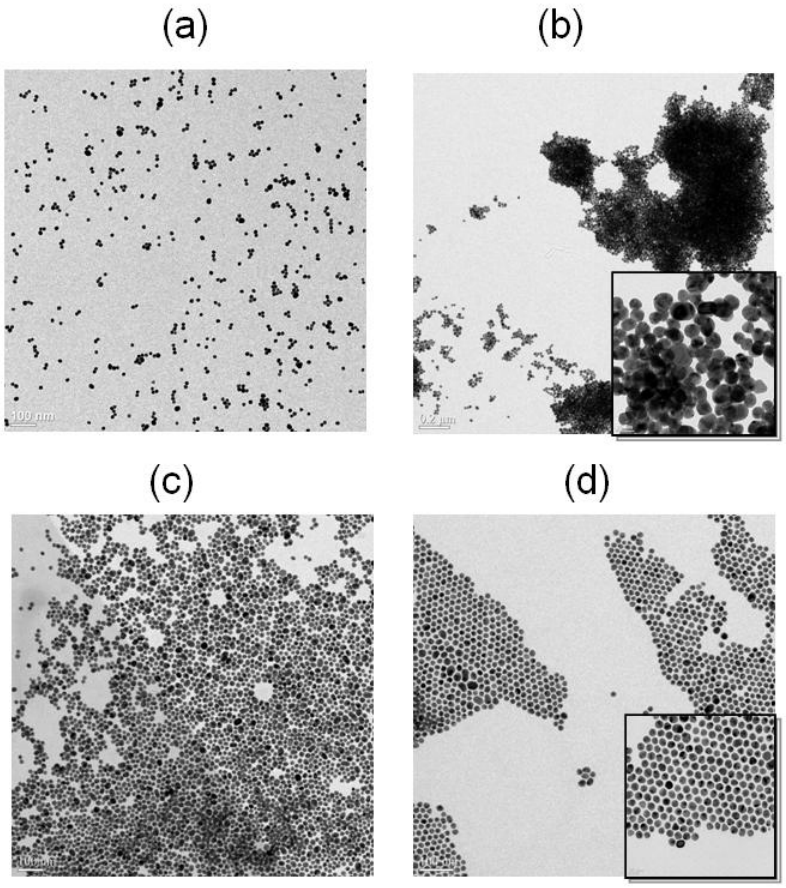

Fugure 1. 1. Transmission electron microscopy graphs of gold nanoparticles with diameter of ca. 17 nm before ligand exchange (a) and after EGMUDE addition at different time intervals: 4 minutes (b), 1 day (c) and 7 days (d). Inset is a magnified part of the corresponding image.

The particles exhibited one narrow absorbance band at 523 nm in the UV-visible spectra which is attributed to the surface plasmon resonance (SPR) band of monodisperse and well separated gold nanoparticles (Figure 1.2a). The dialysis of

citrate stabilized gold colloid was performed to eliminate the byproducts, such as sodium ions, excess citrate and its oxidation product. The purified gold colloid displayed UV-visible spectra with a maximum at 524 nm. No signals were observed in the UV-region that could be attributed to byproducts (excess citrate and its oxidation products). This shows that the latter were successfully removed from the sample during the dialysis (Figure 1.2a). The small broadening of SPR band can be related to slight agglomeration of gold nanoparticles.

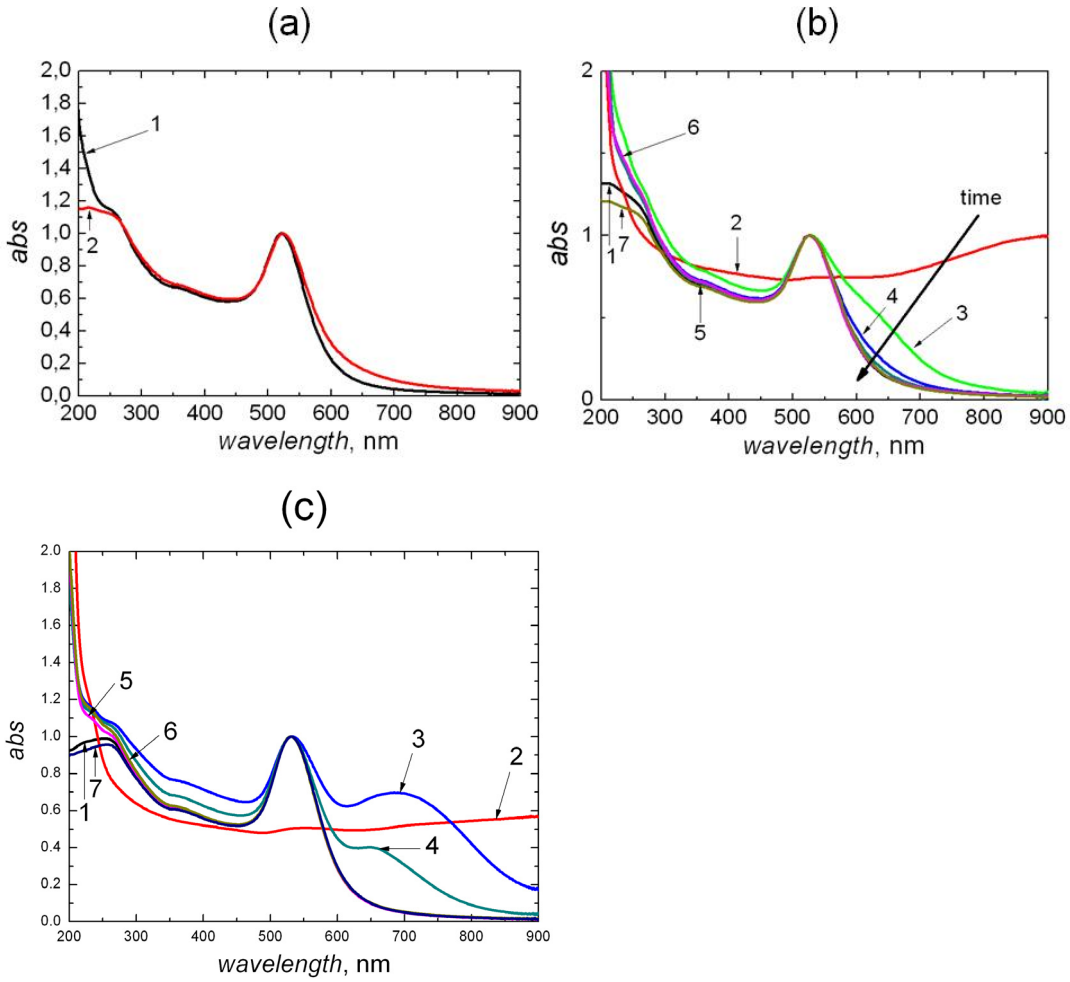

Fugure 1. 2 UV-visible absorption spectra (a) of citrate covered 17 nm gold colloid before (1) and after (2) dialysis, (b) of 17 nm gold colloid before (1) and after EGMUDE addition at different time intervals: after 4 minutes (2), 15 hours (3), 1 day (4), 2 days (5), 7 days (6) and purified with EtOH (7) and (c) of 40 nm gold colloid before (1) and after EGMUDE addition at different time intervals: after 30 minutes (2), 1 day (3), 2 days (4), 3 days (5), 7 days (6) and purified with EtOH (7).

Gold surface modification via triethyleneglycolmono-11-mercaptoundecylether (EGMUDE)

Modification of the gold surface with EGMUDE was carried out by the addition of thiol (EGMUDE) into dialyzed gold colloid in a 1:2.5 Au:thiol molar ratio. EGMUDE was mixed with a small quantity of water forming a turbid solution due to limited solubility of EGMUDE in water. While the EGMUDE was injected, the gold nanoparticles aggregated, which could be easily observed by eyes, and rapidly precipitated (Figures 1.3b,c). Four minutes later almost no absorbtion band could be found in UV-visible spectra shown in Figure 1.2b. The electron micrograph (Figure 1.1b) demonstrates as well very compact and dense aggregates without any separation between particles.

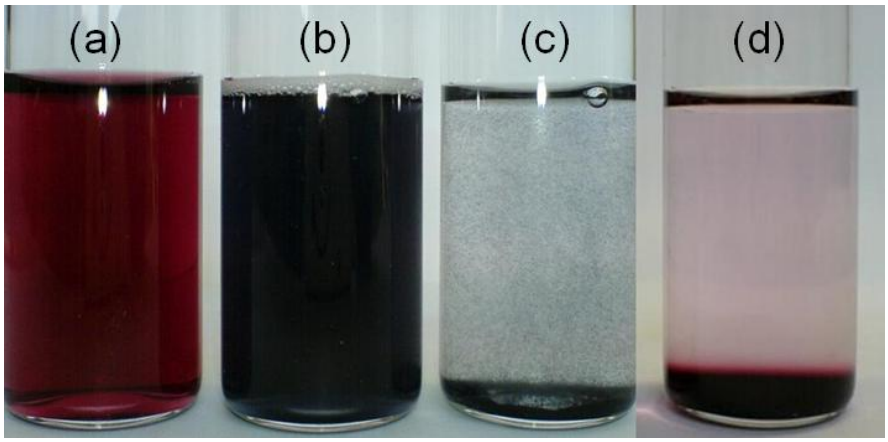

.

Fugure 1. 3 Vials with different gold colloids: a) citrate covered, b) just after EGMUDE addition, c) after 10 min and d) after 1 day.

The position of the surface plasmon band directly reflects the distance between the metal particles[17]. It has been shown that there is a significant shift of the surface plasmon band at relative distances between the nanoparticles d/(2R) (R is the nanoparticle radius, d is the center to center distance) smaller than about 1.4. Therefore, for particles of 17 nm in diameter strong shifts due to the interaction of the plasmons are expected for center to center distances smaller than d = 23.8 nm (= 1.4 x 17 nm), which corresponds to a separation of the nanoparticle surfaces of 6.8 nm (= 23.8 nm – 17 nm). For comparison, the fully extended EGMUDE molecule has a

length of 2.76 nm, as determined by energy minimization using HyperChem. For example, Figure 1.2b shows a secondary plasmon band with a shift of about 100 nm after 15 h. According to the work of Schiffrin and coworkers[17] a shift of 100 nm corresponds to a relative distance d/(2R) of less than 1.1 and therefore a distance between the surfaces of adjacent gold nanoparticles of less than 1.7 nm. This is more than the interparticle distance of 2 x 0.3 nm = 0.6 nm caused by adsorbed citrate ions but significantly less than the distance expected for gold nanoparticles fully covered by EGMUDE but touching each other, where a distance of 2 x 2.76 nm = 5.52 nm is expected, assuming no interpenetration of the two stabilizer layers on adjacent nanoparticles. For the latter distance a shift of less than 20 nm would be expected. It should be noted that these values change quantitatively for different particle sizes. Indeed we observed qualitatively the same phenomena for 40 nm particles (Figure 1.2c) upon functionalization by EGMUDE, however with correspondingly more pronounced shifts of the secondary plasmon band. This is due to the fact that for the 40 nm particles the relative distances d/(2R) are correspondingly smaller due to the larger particle size.

Interestingly, a slightly red-coloured layer above the precipitate was noted one day after ligand addition (Figure 1.3d). The gold nanoparticles "self-redispersed" under a gentle shaking and formed a homogeneous coloured solution. Analysis of the electron micrograph (Figure 1.1c) of the sample one day after EGMUDE addition shows that the gold nanoparticles distribute more homogeneously without any agglomeration. The broadened SPR band appears again (Figure 1.2b) however with a small shift of 3 nm to longer wavelength. It is well known[18, 19] that the exact position of the plasmon band is extremely sensitive both to particle size and shape and to the optical and electronic properties of the medium surrounding the particles. The red-shift of the plasmon band can be explained by an increase in the local refractive index of the surrounding medium of gold nanoparticles i.e. by adsorbed EGMUDE. The secondary plasmon band becomes less pronounced with time (Figure 1.2b 2 days) and after one week it coincides with the one observed for the initial gold colloid except for the slight red-shift by 3 nm due to the adsorbed EGMUDE (Figure 1.2b 7 days). This observation shows that the citrate layers of gold nanoparticles were replaced by new EGMUDE protecting layer, which stabilizes the particles and prevents them from

aggregation. TEM micrograph (Figure 1.1d) shows the gold nanoparticles a week after EGMUDE was added. The particles are well separated from each other and they can form ordered structures on the surface of the TEM copper grid under the pinning effect and entropy-driven ordering tendency upon solvent evaporation[2]. No UV-band in the absorption spectra of the gold colloid purified by ethanol is observed that could be attributed to EGMUDE (Figure 1.2b) showing that the latter was removed from solution during purification.

In order to directly study the cluster formation and further re-dispersion of gold nanoparticles at different time after ligand addition dynamic light scattering measurements were performed.

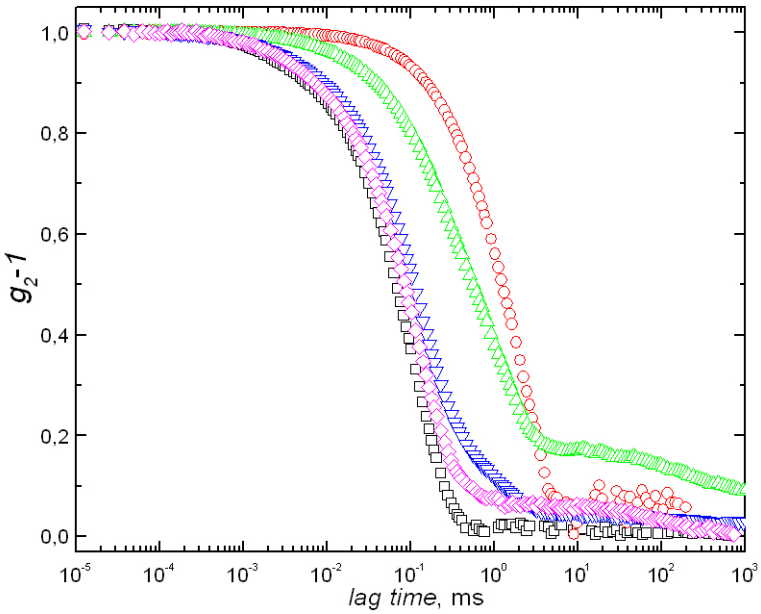

Fugure 1. 4 The normalized electric field autocorrelation functions of gold colloids before ligand exchange (□), just after EGMUDE addition (○), after 1 day (Δ), 3 (∇) and 6 days (◊).

Figure 1.4 shows the correlation functions for the gold colloids at different stages. Initial citrate capped gold nanoparticles exhibit a correlation curve with the smallest decorrelation time and relatively low polydispersity. Cumulant analysis gives a hydrodynamic radius of the particles of around 10 nm. This is slightly larger than

determined from TEM analysis most likely due to the hydrodynamic layer on the particles. EGMUDE solution was directly added into the cylindrical cell containing gold colloid and was kept in the sample chamber for 10 minutes in order to stabilize the temperature. The correlation curve of this sample showed drastic changes with respect to the initial colloid: the decorrelation time shifted to much higher lag times and the baseline became unstable and deviated from zero. Those changes indicate the formation of very large clusters (with hydrodynamic radii larger than 150 nm) usually observed in destabilized suspensions. The sample was afterwards kept in a thermostat for one day and measured again. The correlation curve obtained from this sample exhibited significant shift to the lower lag times due to decreasing of the clusters size. The same tendency was observed for the samples measured even later: The correlation curves of the system approached the one of the initial colloid. The small discrepancy at low intercept close to the baseline arises from a few small clusters in the system. Therefore it can be concluded that after six days the system does not contain large clusters anymore and only individual EGMUDE coated gold nanoparticles are present. The observed self-re-dispersion of the nanoparticles indicates the remarkably high efficiency of the EGMUDE protection.

We considered the possibility that the clusters of gold nanoparticles are organized within the big micelles or the lamellas formed by the EGMUDE, which consists of hydrophilic (triethyleneglycol chain) and hydrophobic (hydrocarbon $C_{11}-$ chain) blocks and which can be considered as nonionic surfactant. Critical micelle concentration (CMC) of EGMUDE is not described in literature but can be estimated by comparison with linear ethoxylate surfactant with a similar structure i.e. triethyleneglycolundecylether (EGUDE). There are several empirical relationships in literature[20-23] to predict CMC for linear alkyl ethoxylates. The CMC of EGUDE which is equal to $1.42*10^{-4}$ mol/l was calculated using the three-parameter empirical model proposed by Ravey[21]

$$\log_{10} CMC = 1.904-0.524C\# + 0.000442C\#*EO\#$$

where C# is the number of carbon atoms in the hydrocarbon chain and EO# is the number of ethylene oxide groups.

The EGMUDE concentration in the gold colloid was $1.27*10^{-3}$ mol/l that was 9 times higher than CMC of EMUDE. Under these conditions the surfactant molecules form assemblies, for example micelles, to reduce system energy. The formation of such assemblies is in fact indicated by TEM measurements (Fig. 1.5).

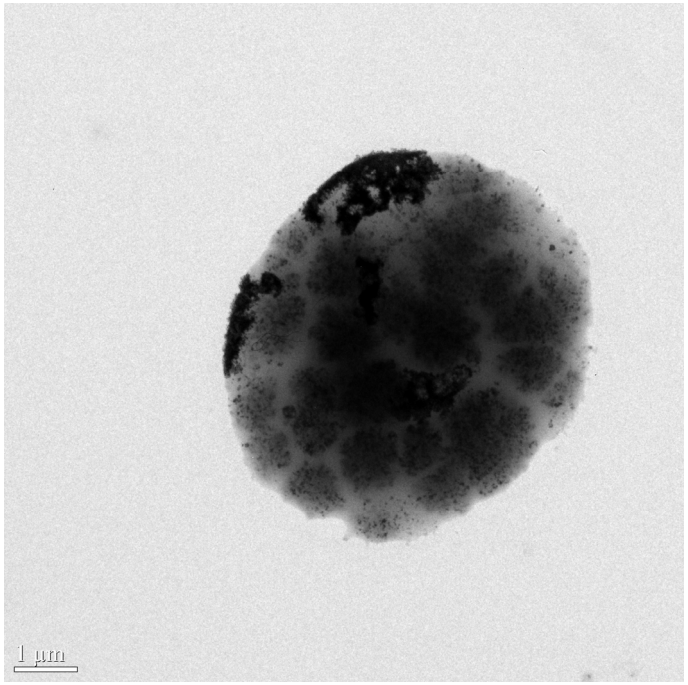

Fugure 1. 5 Transmission electron microscopy graph of the assemblies of EGMUDE and gold nanoparticles, 10 min after ligand addition.

Clearly the EGMUDE-nanoparticle composite shows some hierarchical organization. Within the entire entity with a diameter of about 6 µm domains of about 1 µm are visible with very high local concentration of gold nanoparticles. Similar nanoparticle composite structures have been observed recently when flocculating citrate stabilized gold nanoparticles with a polycation[24]. However, in contrast to our case, the changes observed, for example in the UV-vis spectra, were not reversible. Note that the preparation method of gold nanoparticles presented here relies on the fact that the thiol (EGMUDE) forms micelles in water.

The ligand exchange on the gold nanoparticle surface takes place within these structures and therefore at locally extremely high EGMUDE concentrations. The

ligand exchange process is a critical point with respect to nanoparticle stability. The gold nanoparticles are initially charge stabilized due to the adsorbed citrate. Once the particles are fully covered by EGMUDE they are sterically stabilized. During the exchange there is however a critical point where the charge diminishes but the sterical stabilization is not yet fully established. To avoid agglomeration at this point the exchange is normally done in dilute solutions in order to minimize particle collisions during the critical phase. In contrast, the results presented above show that in our system the exchange is taking place within supramolecular assemblies where the nanoparticle concentration is locally extremely high. This is a strong indication that within these assemblies the EGMUDE leads to an organization of the nanoparticles that prevents them from irreversible agglomeration. The surface functionalization goes hand in hand with a structural change within the composite assemblies. This is clearly indicated by the changes in the UV-vis spectra. The position of the shifted plasmon band shows that at the beginning of the process the distance between fractions of the gold nanoparticles is very small, in agreement with TEM. This distance then increases with time until the particles are fully separated. At the same time the supramolecular assemblies are destroyed (dissolved) as shown by DLS. Reasons for this might be a decrease of the concentration of free EGMUDE in solution due to the binding to the gold nanoparticle surface and/or a destabilization of the assemblies by the functionalized nanoparticles itself.

1.5 Conclusions

In conclusion, we showed that EGMUDE not only acts as stabilizing or protecting agent, but also as reversible flocculator in aqueous medium. Such a combination does not only provide prove of effective stabilization but also allows to directly concentrate the gold colloid by separation of the sediment. Consequently, we can easily produce gold colloid of up to 0.01 vol. %. During the exchange of citrate by EGMUDE the nanoparticles are organized in supramolecular nanoparticle-EGMUDE assemblies, preventing irreversible agglomeration. Furthermore, we demonstrated that the current synthetic protocol is highly valuable to prepare well-dispersed and stable gold colloids.

Acknowledgement

Financial support from the Bundesamt für Berufsbildung und Technologie in the frame of a KTI project is kindly acknowledged.

1.6 References

1 D. L. Fedlheim and C. A. Foss, *Metal Nanoparticles: Synthesis, Characterization and Applications*, CRC Press, Marcel Dekker, Inc; New York, 2001.

2 Y. Yang, W. Wang, J. Li, J. Mu and H. Rong, *J. Phys. Chem. B*, 2006, **110**, 16867-16873.

3 C. J. Zhong and M. M. Maye, *Adv. Mater.*, 2001, **13**, 1507-1511.

4 Y. Kim, R. C. Johnson and J. T. Hupp, *Nano Lett.*, 2001, **1**, 165-167.

5 H. Wohltjen and A. W. Snow, *Anal. Chem.*, 1998, **70**, 2856-2859.

6 J. F. Hainfeld, *Nature*, 1988, **333**, 281-282.

7 G. Schmid and B. Corain, *Europ. J. Inorg. Chem.*, 2003, **2003**, 3081-3098.

8 J. Kimling, M. Maier, B. Okenve, V. Kotaidis, H. Ballot and A. Plech, *J. Phys. Chem. B*, 2006, **110**, 15700-15707.

9 T. Teranishi, S. Hasegawa, T. Shimizu and M. Miyake, *Adv. Mater.*, 2001, **13**, 1699-1701.

10 J. W. Doolittle and P. K. Dutta, *Langmuir*, 2006, **22**, 4825-4831.

11 M. Shena, Y. Dua, N. Huaa and P. Yang, *Powder Techn.*, 2006, **162**, 64-72.

12 C.-H. Su, P.-L. Wu and C.-S. Yeh, *J. Phys. Chem. B*, 2003, **107**, 14240-14243.

13 K. Mallicka, Z. L. Wang and T. Pal, *J. Photochem. Photobiol. A: Chem.*, 2001, **140**, 75-80.

14 N. R. Jana, L. Gearheart and C. J. Murphy, *Langmuir*, 2001, **17**, 6782-6786.

15 G. Frens, *Nature Physical Science* 1973, **241**, 20-22.

16 B. V. Enustun and J. Turkevich, *J. Am. Chem. Soc.*, 1963, **85**, 3317-3328.

17 I. E. Sendroiu, S. F. Mertens and D. J. Schiffrin, *PCCP*, 2006, **8**, 1430-1436.

18 S. Underwood and P. Mulvaney, *Langmuir*, 1994, **10**, 3427-3430.

19 W. Haiss, N. T. Thanh, J. Aveyard and D. G. Fernig, *Anal. Chem.*, 2007, **79**, 4215-4221.

20 P. D. T. Huibers, V. S. Lobanov, A. R. Katritzky, D. O. Shah and M. Karelson, *Langmuir*, 1996, **12**, 1462-1470.

21 J. C. Ravey, A. Gherbi and M. J. Stébé, in *Trends in Colloid and Interface Science II*, Springer, Berlin / Heidelberg, 1988, vol. 76, pp. 234-241.

22 M. J. Rosen, *Surfactants and interfacial phenomena*, *Wiley*, *New Jork*, 1989.

23 P. Becher, *J. Disp. Sci. Techn.*, 1984, **5**, 81 - 96.

24 G. F. Schneider and G. Decher, *Nano Lett.*, 2008, **8**, 3598-3604.

Chapter 2

A study on the thermal conductivity of gold nanoparticle colloids

A study on the thermal conductivity of gold nanoparticle colloids

Authors: Natallia Shalkevich, Werner Escher, Thomas Buergi, Bruno Michel, Lynda Si-Ahmed and Dimos Poulikakos

2.1 Abstract

Nanofluids (colloidal suspensions of nanoparticles) have been reported to display significantly enhanced thermal conductivities relative to those of conventional heat transfer fluids, also at low concentrations well below 1% per volume[1-3]. The purpose of this paper is to evaluate the effect of the particle size, concentration, stabilization method and particle clustering on the thermal conductivity of gold nanofluids. We synthesized spherical gold nanoparticles of different size (from 2 nm to 45 nm) and prepared stable gold colloids in the range of volume fraction of 0.00025 - 1 %. The colloids were inspected by UV-visible spectroscopy, transmission electron microscope (TEM) and dynamic light scattering (DLS). The thermal conductivity has been measured by the transient hot-wire method (THW) and the steady state parallel plate method (GAP method). Despite a significant search in parameter space no significant anomalous enhancement of thermal conductivity was observed. The highest enhancement in thermal conductivity is 1.4% for 40nm sized gold particles stabilized by EGMUDE (triethyleneglycolmono-11-mercaptoundecylether) and suspended in water with a particle-concentration of 0.11 vol%.

Keywords: gold, nanofluids, thermal conductivity, heat transfer

2.2 Introduction

Cooling poses one of the major technical challenges facing many industrial sectors such as transportation, microelectronics and power generation. The common trend to address this problem is to enlarge surface of the heat sink by, for example, incorporating mirco-channels into the heat transfer structure[4-6]. However, the performance of such systems could be further increased if one could engineer novel fluids, which provide superior thermophysical properties to conventional fluids. Metals and metal oxides have much higher thermal conductivity than common fluids. Therefore, an innovative way to elevate the thermal conductivity of fluids is the addition of nanometer-sized metal or metal oxide particles into a base fluid. The use of nanometer-sized particles with large specific surface area could not only improve the heat transfer but also provides higher stabilization against particle sedimentation and prevent clogging of the heat sink. Various types of nanoparticles such as metallic[1-3, 7, 8], non-metallic[9-14], with different shapes and sizes, can be suspended in different fluids forming so-called nanofluids.

A number of the experimental studies on thermal properties of nanofluids show very large enhancements in the thermal conductivity of nanofluids. The most extreme results were obtained for different allotropes of carbon. For example, enormous enhancements of thermal conductivity by 160% and by 70% were observed for a suspension containing 1% of MWCNTs in oil[13] and for 1% ultra-dispersed diamond in ethylene glycol respectively[14]. Nevertheless those materials are not very stable even at moderate concentrations and need to be studied more carefully in different media.

A variety of oxide particle suspensions were also investigated[9-14]. Due to the moderate thermal conductivity of solid oxides they require high volume fractions (>5%) to achieve significant thermal conductivity enhancements. The high particle concentrations implicate problems of increased viscosity and colloidal instability which make those suspensions inapplicable for convective heat transfer.

In some cases aqueous nanofluids at vanishing concentrations of “naked” metallic particles such as 50-100 nm copper at 0.001 volume fraction[2] and 10-20 nm gold at 0.00026 vol%[3] were reported to yield thermal conductivity enhancements by

up to 23.8% and 21% (at 60 °C) respectively. On the other hand, several other studies demonstrated just moderate, expected enhancements of thermal conductivity for similar fluids. S. A. Putnam et al.[1] showed that the enhancement of thermal conductivity was only 1.3% for 4 nm Au particles suspended at 0.35 vol% in ethanol. The contradictory experimental data, reporting anomalous thermal conductivity enhancements could be attributed to poor consideration of particle morphology, size distribution, colloidal stability or systematic errors in measuring the fluids thermal conductivity.

In this paper a systematic effort was made to produce and to characterize aqueous gold nanofluids. We varied the particle size, the particle loading and the stabilization method. The gold colloids were characterized by UV-visible spectroscopy, TEM and DLS in order to determine the particle size, morphology and the stability of the colloid. The thermal conductivity measurements were carried out using two independent techniques, namely the transient hot-wire method and the static heated plate method, to eliminate any systematic errors due to the measurement method itself.

2.3 Experimental section

2.3.1 Materials

Hydrogen tetrachloroaurate (III) solution (4.36 M) and silica stabilized gold nanoparticles were supplied by Metalor Technologies SA, Neuchâtel, Switzerland. Trisodium citrate dihydrate (99%), N-acetyl-L-cysteine (99%), L-glutathione reduced (98%), tetramethylammonium hydroxide (0.1M in water), triethyleneglycolmono-11-mercaptoundecylether (95%) (EGMUDE), and aqueous solution of thiol stabilized gold nanoparticles (3-5 nm of diameter, 0.1 vol%) were purchased from Sigma-Aldrich. Ethanol (99.9%) was purchased from Merck. Methanol (99.9%) and sodium borohydride (99%) were purchased from Acros. Glacial acetic acid was purchased from Carlo ERBa. All reagents were used as received. Milli-Q (Millipore) water with a resistivity of 18.2 MΩ was employed throughout. Dialysis membranes (3.5 kDa, Spectra/Por CE) and filtration membranes (0.2 μm, PTFE) were obtained from Spectrum and from Sigma-Aldrich respectively.

2.3.2 Instrumentation

UV-visible spectra (200-900 nm) were recorded on a Cary 300 spectrometer using a quartz cell of 1 cm path length.

Transmission electron micrographs (TEM) were obtained with a Philips C 200 microscope in bright field mode at a voltage of 200 kV. The samples for TEM study were prepared by casting a few drops of the gold colloid onto carbon-coated copper grids (300 mesh) and used after solvent evaporation in air.

Dynamic light scattering (DLS) was performed with an ALV-5000 spectrophotometer equipped with an argon-laser (Coherent, model Innova 300, λ = 488 nm), a digital auto-correlator (ALV) and variable angle detection system. Measurements were made at a fixed scattering angle of 90° and a temperature of 25.0 ± 0.1 °C. The individual correlation functions were analyzed using a second-order cumulate fit. The DLS data were also analyzed with the CONTIN method to obtain the inverse Laplace transformation of the autocorrelation function and the distribution of decay times Γ. The CONTIN data were converted into intensity weighted distributions of hydrodynamic radius.

2.3.3 Gold colloids with the particle size in the range of 1-3 nm

Spherical gold nanoparticles with diameter of 1-3 nm were prepared using the Brust technique in a single-phase system[15] where an Au(III) chloride salt was mixed with a thiol RSH in a suitable solvent, and subsequently reduced with sodium borohydride $NaBH_4$. Before the reduction step, the thiols were oxidized by gold(III) ions forming Au(I)-SR polymers[16, 17]:

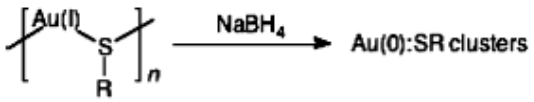

Figure 2. 1. Schematic of synthesis of Au:SR nanoparticles by chemical reduction of Au(I)-SR polymers with $NaBH_4$

The $HAuCl_4$:RSH molar ratio which controls the average core size was equal to 1:4 for the two syntheses described next.

2.3.3.1 Synthesis of glutathione protected gold nanoparticles (Au_2nm-SG)

Glutathione (GSH) protected gold NPs were prepared following a previous report[18]. 0.25 mmol of $HAuCl_4$ was added to 50 ml of methanol followed by 1 mmol of glutathione. The solution was cooled in an ice bath for 20 min. 2.5 mmol of $NaBH_4$ was dissolved in 12.5 ml of water that was preliminary cooled to 0 °C and then it was injected rapidly into methanol solution under vigorous stirring. After, the mixture was allowed to react for 90 min in the ice bath. The resulting precipitate was filtered using 0.2 μm PTFE membrane and washed with methanol to remove impurities. The collected precipitate was dissolved in water and the solvent was removed under vacuum at ≤ 40 °C. The cleaning procedure was repeated several times. Finally, glutathione stabilized gold particles were dialyzed in water during 5 days with replacing water every 10 hours. The dialyzed solution was finally evaporated under vacuum resulting in a black powder.

2.3.3.2 Synthesis of N-acetyl-L-cysteine protected gold nanoparticles (Au_2nm-NAC)

Gold nanoparticles stabilized by N-acetyl-L-cysteine (NAC) were prepared by a procedure described by *Gautier et al.*[19]. 1 mmol (163 mg) of N-acetyl-L-cysteine and 0.25 mmol of $HAuCl_4$ were dissolved in 50 ml of 6:1 methanol:acetic acid mixture giving a cloudy white suspension. This is attributed to the formation of Au(I)-NAC polymer. Acetic acid was used to prevent the deprotonation of thiol. 17.5 ml of cold freshly prepared aqueous $NaBH_4$ solution (10 mmol) was carefully added to the Au(I)-NAC polymer solution under vigorous stirring. The black suspension was fast formed and stirred for another 90 min. The precipitate was filtered through the 0.2 μm PTFE membrane, washed with ethanol, dissolved in water and dried under vacuum at T ≤ 40 °C. After a series of precipitation—filtration (with ethanol) cycles the complete purification of the product was accomplished by dialysis in water over the course of 5

days. The water was changed every 10 hours. Final gold colloid was evaporated under vacuum giving a black powder.

The gold colloids with volume fractions up to 1 vol% can be easily prepared through the addition of the powder to a solvent and ultrasonic treatment for 15 min. The resulting solutions are also stable with some content of organic solvent (≤ 25 vol%) such as methanol, isopropanol, propylene glycol, and stay homogeneous after two hours of heating (≤ 80 °C).

2.3.4 Gold colloids with nanoparticles larger than 16 nm in diameter

2.3.4.1 Synthesis of citrate stabilized gold nanoparticles

The data for the syntheses of gold colloids with the 16-40 nm gold particles are presented in the Table 2.1.

Spherical gold nanoparticles from 16 to 40 nm in diameter were prepared by citrate reduction of Au(III) as described by Turkevich and Frens[20, 21]. In this method, a small amount of $HAuCl_4$ (*x* mmol) was dissolved in 50 ml of water and heated to the boiling. 1.25 ml of sodium citrate solution with *y* mmol of the reductant was rapidly introduced into boiling gold solution under continuous heating and vigorous stirring. A color change from pale yellow over colorless to red-wine (or more violet) took place within 15 s. The mixture was kept boiling for 15 min and then cooled to room temperature. The reaction is quite fast, thus the particle size as well as polydispersity depend on many synthesis conditions such as the Au:citrate molar ratio, the concentrations of precursors, the rate of addition of precursors or the temperature of reaction mixture. In our case, the monodispersed gold nanoparticles with different size were synthesized by changing the Au:citrate molar ratio and the concentration of precursors (see Table 2.1).

Table 2.1. Synthesis conditions for gold colloids

sample	*x* ($HAuCl_4$), mmol	*y* (citrate), mmol	Au:thiol molar ratio	C_M (Au), mM
Au17-cit	0.028	0.084		0.55
Au17-cit	0.0125	0.0375		0.25
Au40-cit	0.0125	0.0221		0.25
Au17-SG*			1:5	0.11
Au17-EGMUDE**			1:2.5	0.55
Au17-EGMUDE			1:2.5	0.55
Au40-EGMUDE**			1:2.5	0.82
Au40-EGMUDE			1:2.5	0.89

(*) ligand exchange at pH~9 through an addition of the tetramethylammonium hydroxide (TMeAOH)

(**) ligand exchange via reversible formation of gold nanoparticle-EGMUDE composite assemblies.

2.3.4.2 Surface modification of gold nanoparticles and preparation of concentrated gold colloids

Gold colloids were purified before ligand exchange generally via dialysis. For this, 50 ml of citrate stabilized gold colloid was placed in a 3.5 kDa membrane and dialyzed against water which was changed every 10 h during a week. In several cases (Au_40nm-EGMUDE) an ultra filtration technique was used to purify and concentrate the gold colloid. UV-visible spectra analysis and the pH control of gold colloid were used to determine the end of colloid purification by dialysis or by ultra filtration.

Two hydrophilic stabilizers glutathione and triethyleneglycol-11-mercaptoundecylether (EGMUDE) were used to modify the surface of 17 nm gold

nanoparticles via reactive thiol groups. The 40 nm gold nanoparticles were covered by EGMUDE.

Typically, the modification of the gold particle surface was carried out by an addition of aqueous solution of ligand to citrate stabilized gold colloid in a respective Au:thiol molar ratio (see Table 2.1). The resulting colloid was vigorously stirred for 2 hours and then kept for several days for the complete ligand exchange. The modified colloid concentrated by rotary evaporation under vacuum at $T \leq 40\ ^{\circ}C$ giving concentrated gold solution or black powder. Concentrated gold colloids were purified via dialysis against water (see above) while the powders were repeatedly washed with a small quantity of ethanol to remove the excess of thiol and redispersed in a small volume of water or of water-alcohol mixture.

The EGMUDE capped gold colloids (marked by **) with a different particle size were prepared otherwise i.e. via reversible formation of gold-surfactant composite assemblies that was described in a previous report[22]. Briefly, a colloidal (micellar) solution of EGMUDE in water (0.07 mmol in 5 ml) was added to the dialyzed gold colloid (50 ml, 0.55 mM) under stirring. The color of the mixture quickly turned to black and a complete particle precipitation took place within 15 min. After few days without stirring, the gold nanoparticles were successfully self-redispersed forming a homogenous colloid. The solvent was removed under vacuum at $T \leq 40\ ^{\circ}C$. The gold nanoparticles were washed with ethanol and redispersed in water.

2.3.5 Thermal conductivity measurements

We utilized different techniques to measure the thermal conductivity of electrical conducting liquids. We implemented a static heated plate and a transient hot wire method to eliminate any systematic errors due to the measuring method itself. Additionally, the static heated plate setup requires a smaller fluid volume, which is advantageous for a fast screening of different nanofluid parameters.

The transient hot wire method typically employs a metal wire, immersed into a liquid. The liquid and the metal wire are initially in thermal equilibrium. The wire is exposed to a step voltage resulting in a constant heat generation along the wire. The

transient rise in the wire temperature depends on the thermal conductivity of the surrounding liquid whereas the wire temperature is typically measured by the change of electrical resistance. The wire away from its ends behaves like an infinite line heat source surrounded by an infinite volume of liquid. The thermal conductivity of the fluid, λ, can be determined by

$$\lambda = \frac{\dot{q}'}{4\pi\left(T_2 - T_1\right)} \ln\left(\frac{t_2}{t_1}\right), \qquad [2.1]$$

where $\dot{q}'$ is the heat generation per unit length and T_2 and T_1 are the absolute temperatures at the time t_2 and t_1 respectively.

The present transient hot wire cell was adapted from the design being proposed by Assael et al. in a series of papers [23-25] (see Figure 2.2a). A 25 μm thick tantalum wire was used as the heating and sensing wire. We used 500 μm thick tantalum wires as supporting leads to keep the wire in tension and as electrical connections. The wires were electrically insulated from the test fluid by *in situ* anodization whereby a Tantalum pentoxide layer of about 70 nm was formed at the surface of the wires. A positive bias was applied between the Tantalum wires and the fluid vessel to stabilize the insulating oxide layer. This arrangement also provided the means to observe the leakage current between the wire and the fluid vessel and hence to observe any changes in the quality of the oxide layer.

We used a two wire approach in order to automatically compensate for axial heat conduction at the wire ends. Th this end, the resistance change of a 20 mm long wire was subtracted from the resistance change of a longer wire being 50 mm in length. This was achieved by connecting each wire to one arm of a Wheatstone bridge. Thus, effectively the resistance change of a 30 mm long segment of an infinite long wire was measured. We directly calibrated the temperature dependence of the resistance of the 30 mm long segment and found a coefficient of 0.0031 K^{-1}, being close to tabulated data for tantalum (0.0036 K^{-1}).

The fluid vessel was made of stainless steel with an inner diameter of 15 mm and a length of 90 mm. The dimensions of the fluid vessel were verified by numerical simulation to ensure that the fluid vessel did not influence the transient temperature

response of the sensing tantalum wire. The total required fluid volume for one measurement amounts to 18 ml. To control the fluid temperature, the fluid vessel was surrounded by a water jacket.

We measured the wire resistance before heating by applying an input current of 3 mA. Afterwards, the wire was heated in a constant voltage mode, whereas the voltage was adapted to the fluid properties to produce temperature rises between 3 K and 4 K in a measurement period of 1.5 s. The transient temperature rise of the wire was measured at a sampling rate of 500 Hz by a digital multimeter. We performed 10 iterations to determine thermal conductivity of a sample within a standard deviation of less than 0.5%. The absolute maximum error was determined by thermal conductivity measurements of water, water/ethanol mixtures and ethanol in a temperature range of 298 K – 323 K and is specified to be less than 2.5% (see Figure 2.2b).

The static heated plate method is based on Fourier's law of heat conduction. We generate a one dimensional heat flux across a thin fluid layer. If the temperature difference across the fluid layer, ΔT, the thickness of the fluid layer, L, and the heat flux per unit area, $\dot{q}''$ are known, we can compute the thermal conductivity of the fluid from,

$$\lambda = \frac{\dot{q}''L}{\Delta T}. \qquad [2.2]$$

A schematic of the static heated plate methods is shown in Figure 3a. The heating was provided by a thin film heater called "Cobra" deposited on the back of a 21 x 21 x 1 mm^3 silicon die. Three temperature sensors were deposited at the same time. The heat flowed downward through a 20 mm diameter, 20 mm long copper piece where two 0.5 mm diameter K-type thermocouples had been embedded. At the end of the copper part, the heat flowed through the liquid layer into a second copper piece, similar to the first one. A Mikros cooler connected to a chiller functioned as heat sink. A glass-ceramic (Macor®) cylinder provided at the same time thermal insulation for the copper pieces and containment for the liquid enclosed between the two copper slugs and the glass-ceramic. Two o-rings provided the required sealing around the copper parts.

The liquid was introduced through a capillary tube glued to the Macor® part. A

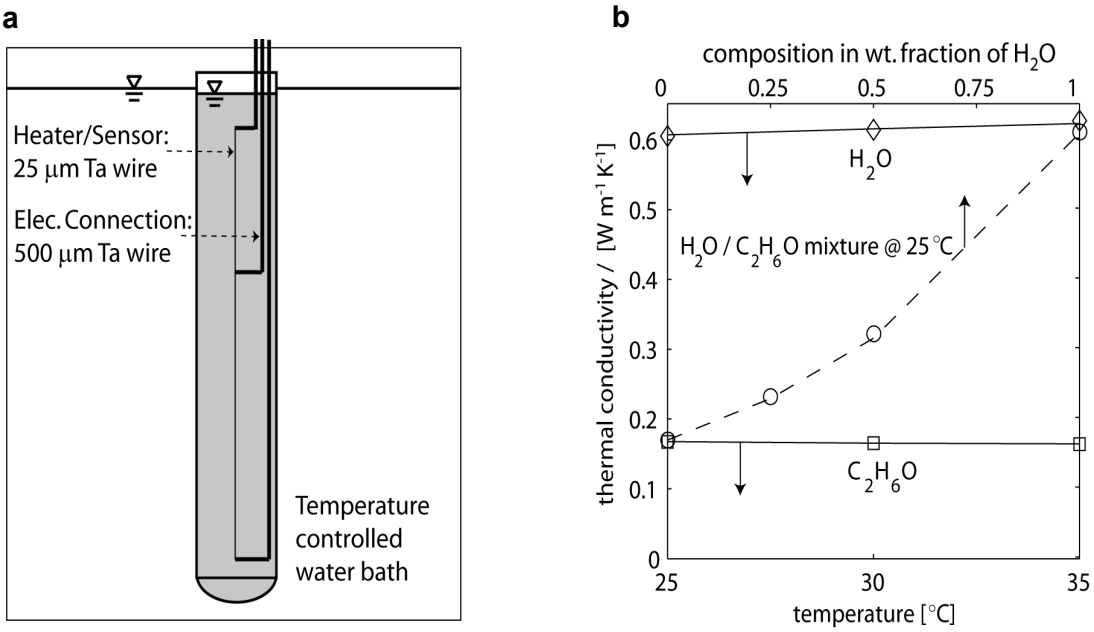

Figure 2.2. (a) Schematic of transient hot wire cell – (b) thermal conductivity of ethanol and water at different temperatures and thermal conductivity of water/ethanol mixtures at different concentrations measured with present transient hot wire cell, markers indicate the measured values and lines reference data from literature (H_20 and C_2H_6O data extracted from NIST Standard Reference Tables, data for fluid mixtures extrapolated from Assael et al.[25]).

second tube functioned as drain for the trapped air. The minimum fluid volume for one measurement was determined to be 2 ml.

The gap between the two copper pieces was measured by four linear variable differential transformer calipers and could be adjusted with 4 screws. In our experiments we chose gab dimensions between 200 – 300 μm. Natural convection was suppressed as the heat flowed from the top to the bottom and a bull's eye level was used to assure that the set up was kept in a horizontal position. In any event, the Rayleigh number of the present apparatus was always kept much smaller than the critical value of 1700.

During a measurement, a constant heat flux of about 20 - 30 W was applied and the temperature profiles in both copper slugs were measured. Assuming a linear temperature profile within the copper cylinders, the temperatures at the solid fluid interface could be interpolated. Hence, if steady state conditions were established, the thermal conductivity of the fluid could be calculated according to equation.

Due to thermal expansion of the system, the exact gap between the copper cylinders could not be determined by the calipers, hence, we used this distance as a calibration factor and corrected for the distance to match the thermal conductivity of water. The error of the method was determined by test measurements with water/ethanol mixtures and ethanol and was identified to be less than 3% (see Figure 2.3b).

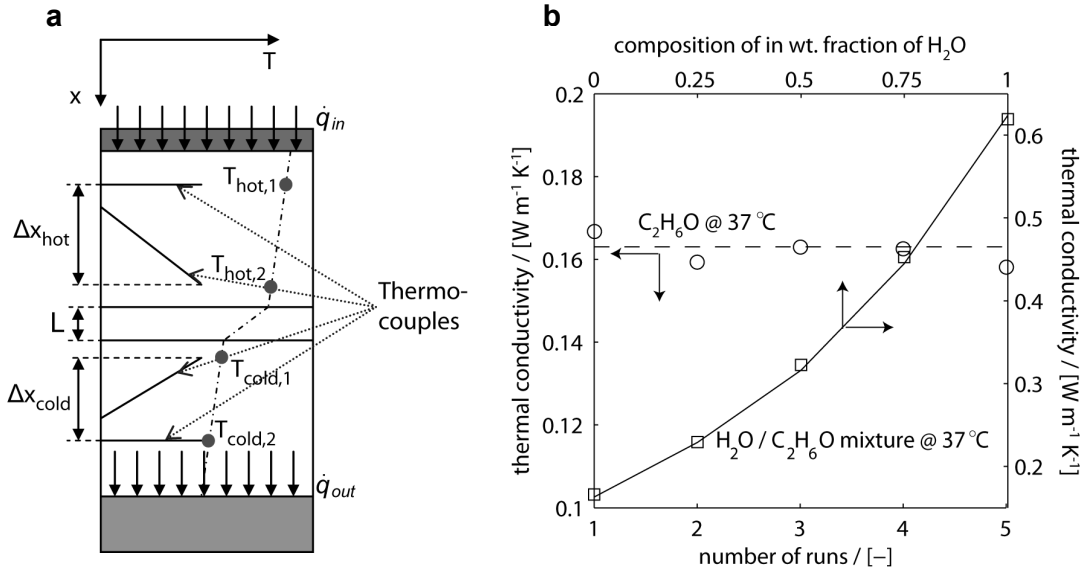

Figure 2.3. (a) Schematic static heated plate set up – (b) thermal conductivity of ethanol and of water/ethanol mixtures at different concentrations measured with present static heated plate method at 37 °C, markers indicate the measured values and lines reference data from literature (C_2H_6O data extracted from NIST Standard Reference Tables, data for fluid mixtures interpolated from Assael et al.[25]).

2.4 Results and discussion

Preparation of gold nanofluids

Spherical gold nanoparticles of sizes from 2 nm to 40 nm were synthesized in water or water-alcohol mixture by reduction of gold (III) salt. The particle size has been controlled by varying the reducing agent (and/or stabilizer)/gold ratio. Typical TEM micrographs of gold nanoparticles with different sizes are shown in Figure 2.4.

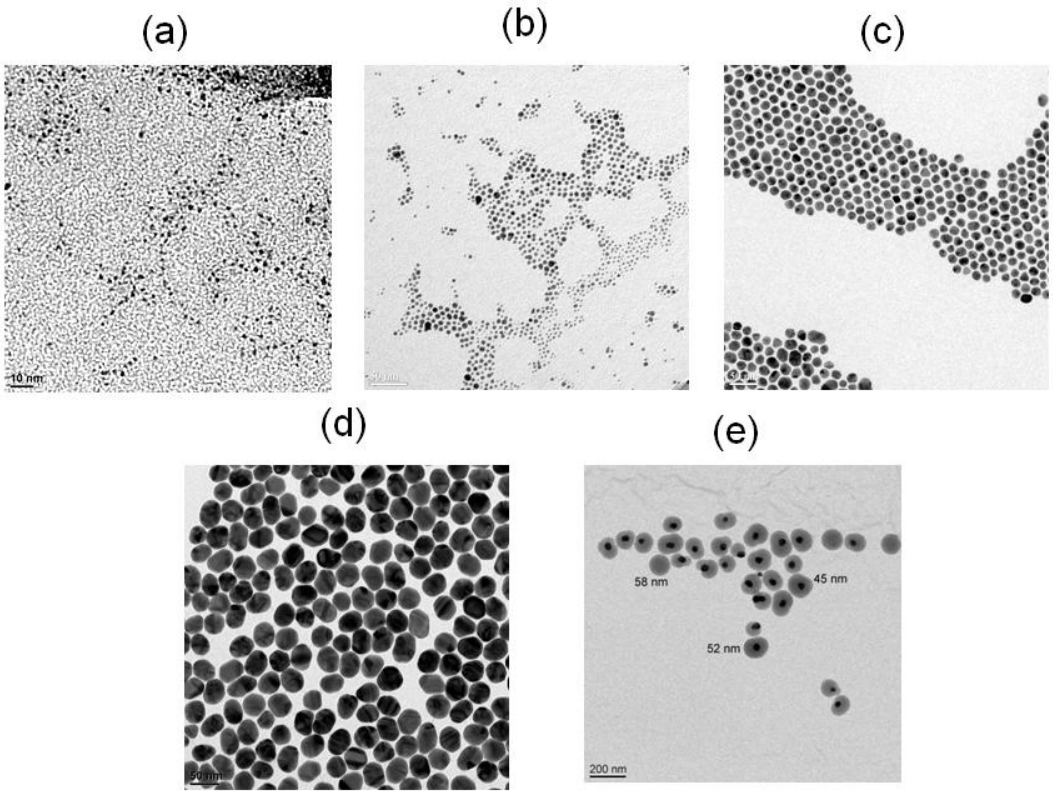

Figure 2.4. Transmission electron microscopy graphs of gold nanoparticles of different size: (a) Au-SG nanoparticles with an average diameter of 2 nm, (b) Au-EGMUDE nanoparticles with diameter of 4 nm, (c) of 17 nm, (d) of 40 nm and (e) Au-silica nanoparticles with a 45 nm in gold core.

The gold particles of 2 nm (Figure 2.4a) have been produced in powder form. The nanopowders have been extremely stable and did not show any signs of decomposition, such as loss of solubility or particle growth, even in a year of storage at ambient temperature in air. The powder was dispersed in water or water-methanol mixture giving homogeneous concentrated colloids. This way allows us to obtain extraordinary concentrated stable gold colloids with volume fraction up to 1 vol%. The stability of highly concentrated colloids with small gold nanoparticles can be attributed to combined charge and steric protection provided by hydrophilic GSH or NAC layers on the gold surface.

The gold nanoparticles with diameter more than 16 nm (Figure 2.4c, 2.4d) were synthesized by citrate reduction forming the stable Au-citrate colloids at volume

fraction less than 0.00055 vol%. Concentrated colloids of the Au-citrate nanoparticles cannot be directly achieved, because of agglomeration and precipitation due to insufficient protection of gold surface by citrate ions. In order to produce more concentrated nanofluids with large and heavy gold particles the steric stabilization of gold surface is most importantly required. Several hydrophilic stabilizers with thiol head group and a hydrophilic part were used to modify the surface of gold-citrate nanoparticles and enhance nanoparticle stability. Ligand exchange with GSH and EGMUDE resulted in concentrated 17 nm gold colloids at 0.0036 vol% and 0.33 vol% respectively. Both concentrated gold colloids contained small amount of the precipitate that could be due to incomplete replacing of citrate by GSH and EGMUDE.

The highly concentrated colloids of 17 nm and 40 nm gold nanoparticles stabilized with EGMUDE were successfully produced by the method of reversible formation of gold-surfactant composite assemblies described in detail elsewhere[22]. This method directly gives very stable particles at high concentration (up to 0.4 vol%). Efficient surface coverage results in concentrated suspension which remaind stable even at high temperature (up to 70 ˚C).

Thermal properties of gold nanofluids

Experimental data for the relative thermal conductivity of different gold nanofluids are summarized in the Table 2.2. Water and methanol-water mixture were used to prepare the nanofluids which could be utilized as coolants for microelectronic devices. Water was chosen because of its excellent thermophysical properties, i.e. low viscosity, very high specific heat and high thermal conductivity. However, the high freezing point and the thermal expansion under freezing confine the temperature work range of water in closed systems. Addition of methanol up to 24% decreases the freezing point of water to - 19.1 ˚C[26] but simultaneously reduces the heat transfer capacity and increases the viscosity of fluid. Nevertheless, methanol seems a suitable water-miscible solvent to decrease the freezing point of water.

For each sample, the thermal conductivity of the reference fluid was measured independently at the same temperature as the gold nanofluid. The temperature of

measurement was varied between 25 °C and 40 °C. Stabilizer was added in the reference fluid (water or water-methanol mixture) to consider its influence on the thermal conductivity of the suspension. The stabilizer amount was taken equal to the quantity of stabilizer adsorbed on the gold particle surface.

The gold nanoparticles were stabilized in different ways. The gold-citrate nanoparticles have charge stabilization due to physically absorbed citrate ions on the gold surface. Such nanoparticles, usually named as "naked" particles, form stable nanofluids only at volume fractions less than 0.001 vol%. Therefore, the stable concentrated colloids require a replacement of citrate by a more sufficient stabilizer. The surface modification was performed by chemical covering (with thiols and silica) of gold particles in order to improve particle stability and to gain highly concentrated gold colloids.

The gold nanofluids in the particle (core) size range from 2 nm to 45 nm and at volume fraction from 0.00025 vol% to 1 vol% were prepared and tested.

Table 2.2. Thermal conductivity of gold colloids

Particle size, nm	stabilizer	Base fluid	Particle volume fraction, %	Relative thermal conductivity	Method of measurement
2	NAC	methanol/water	0.1	0.996 (39 °C)	GAP
			0.2	0.990 (39 °C)	GAP
			1	0.952 (39 °C)	GAP
	GSH	methanol/water	0.1	1.01 (39 °C)	GAP

			0.2	0.989 (39 °C)	GAP
			1	0.959 (39 °C)	GAP
4	EGMUDE	water	0.1	0.997 (37 °C)	GAP
17	citrate	water	0.00025	1.013 (25 °C)	THW
			0.00025	0.997 (40 °C)	THW
			0.00025	1.004 (39 °C)	GAP
			0.00055	1.015 (25 °C)	THW
			0.00055	1.01 (40 °C)	THW
	GSH	water	0.0036	0.998 (33 °C)	GAP
	EGMUDE**	methanol/water	0.008	0.977 (25 °C)	THW
	EGMUDE**	methanol/water	0.018	0.972 (25 °C)	GAP
	EGMUDE**	methanol/water	0.07	0.992 (25 °C)	GAP
	EGMUDE	water	0.33	1.013 (25 °C)	GAP
40	EGMUDE**	water	0.078	1.006 (37 °C)	GAP
	EGMUDE	water	0.11	1.014 (37 °C)	GAP
45	Silica	water	0.4	1.002 (25 °C)	THW

Figure 2.5 shows the effect of volume fraction on relative thermal conductivity of gold colloids. Most of the nanofluids were tested by the GAP method as it requires less fluid volume. Commonly, the tendency of thermal conductivity enhancement with increase of nanoparticle concentration is observed. However, the tested fluids showed only small changes of thermal conductivity being within the range of the measurement uncertainty. The nanofluids consisting of the Au-EGMUDE particles with diameter of 17 nm or 40 nm have a small thermal conductivity enhancement at volume fraction larger than 0.07 vol%. The highest gain of thermal conductivity was observed for Au_40nm-EGMUDE colloid with 0.11 vol %. Several gold nanofluids were tested by both the GAP and the THW methods and no appreciable difference between thermal conductivity values for the same nanofluid measured with the two methods was observed.

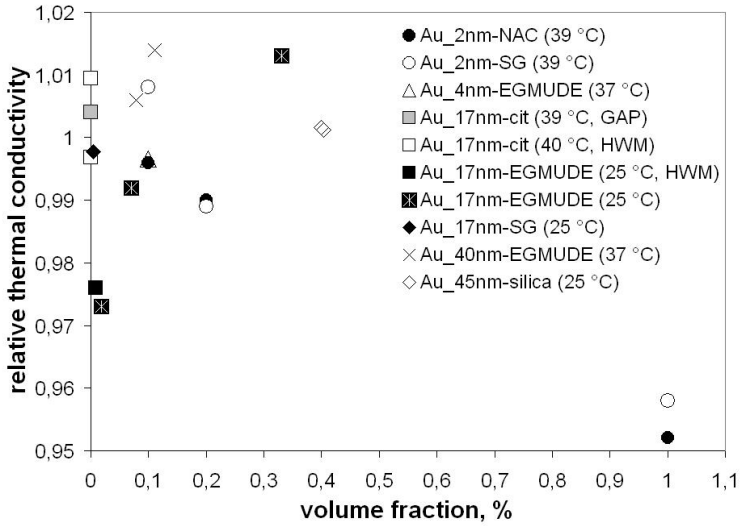

Figure 2.5. Relative thermal conductivity of gold nanofluids as a function of volume fraction.

Surprisingly, the smallest nanoparticles with diameter of 2 nm exhibit even an inverse tendency and thermal conductivity decreasing with increasing of volume fraction. Thus, the nanofluids of Au_2nm-SG and of Au_2nm-NAC particles at maximum concentrations (1 vol%) have the relative thermal conductivities of 0.959 and 0.952 respectively i.e. thermal conductivity lower than for basefluids (0.636 W/(m*K) and 0.635 W/(m*K) respectively).

Such "negative" tendency for very small particles can be explained by two factors. The first one is the discrete nature of subnanometer gold particles[27] i.e. the presence of discrete energy levels in the electronic structure of metal nanocrystals. The level pattern near the highest occupied level is critically sensitive to size and shape of the metal crystallite and essential to describing its properties (thermal, chemical, electrochemical)[28] and that might account for lower thermal conductivity of subnanometer particles. Secondly, the stabilizer layer can act as thermal insulator because of its low thermal conductivity. The stabilizer effect can be assessed through a calculation of Au/stabilizer molar and volume ratio for a spherical gold particle with well-packed monolayer of stabilizer (see Table 2.3). Here, the length of the individual EGMUDE molecule in fully extended mode was taken as 2.76 nm and the average thickness of NAC and GSH monolayers were assumed as 0.61 nm and 0.92 nm respectively.

Table 2.3. Stabilizer content in covered gold nanoparticles.

Diameter, nm	Kind of stabilizer	Au/stab molar ratio	Au/stab volume ratio
2	GSH	6.7	0.165
2	NAC		0.315
2	EGMUDE	5.94	0.019
4	EGMUDE	11.9	0.08
17	EGMUDE	50.5	0.755
40	EGMUDE	118.9	2.11

The Au/stabilizer volume ratios are much less than 1 despite reasonably high molar ratio. Therefore, we can treat the 2 nm gold nanoparticles as partially isolated for heat transfer.

Figure 2.6 presents the relative thermal conductivity as a function of particle size. Indeed, there is a clear tendency of decreasing thermal conductivity with decreasing particle size in the range of 2-40 nm. A similar tendency was observed for alumina nanoparticles dispersed in ethylene glycol. Xie et al.[29] reported a doubled enhancement of thermal conductivity for the 60 nm alumina particles as compared to the 15 nm particles. That contradicts to the commonly stated influence of particle size i.e. the improvement of thermal conductivity due to increased specific surface area of the dispersed phase.

The importance of the shell composition to the heat transfer can be illustrated as well by the data for 17 nm particles (see Figure 2.6). We have tested three kinds of surface modifiers i.e. the citrate, glutathione (GSH) and EGMUDE. The latter two are chemically bound to the gold surface, whereas the former enables charge stabilization of the gold nanoparticles. The gold-citrate nanofluid at 0.00055 vol% exhibits thermal conductivity enhancement in the same range as nanofluids with EGMUDE modified particles, even though the latter had a 600 times higher concentration. The system with glutathione as a modifier even reveals the same thermal conductivity as basefluid (0.622 W/(m*K)).

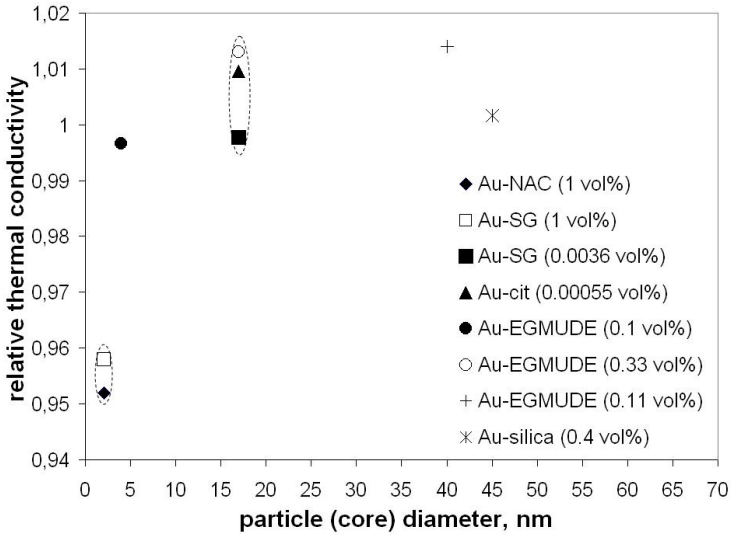

Figure 2.6. Relative thermal conductivity of gold nanofluids as a function of particle size.

The chemical nature of the nanoparticle shell plays an important role for heat transfer. Min Hu et al.[30] demonstrated higher heat dissipation rates for 15 nm silica coated gold nanoparticles, compared to citrate stabilized gold particles even when the silica layer is thicker than 10 nm. Therefore, we prepared and tested 45 nm gold nanoparticles with 40 nm silica coating (see Figure 2.4e). Unfortunately, no thermal conductivity enhancement was observed for silica stabilized 45 nm gold nanofluid at 0.4 vol%. That could be attributed to the properties of the silica shell which depend on the production and processing of the silica shell. The highest cooling rates should be obtained for shells that are well formed and have thermal properties that are close to fused silica. Porous shells that have a significant solvent penetration will have lower cooling rates [30].

The citrate stabilized nanofluid agrees in terms of particle material, size and morphology with a previous published study of Patel et al.[3]. Furthermore, the colloids are prepared and stabilized by the same procedure. A comparison of the obtained thermal conductivity is summarized in figure 2.7.

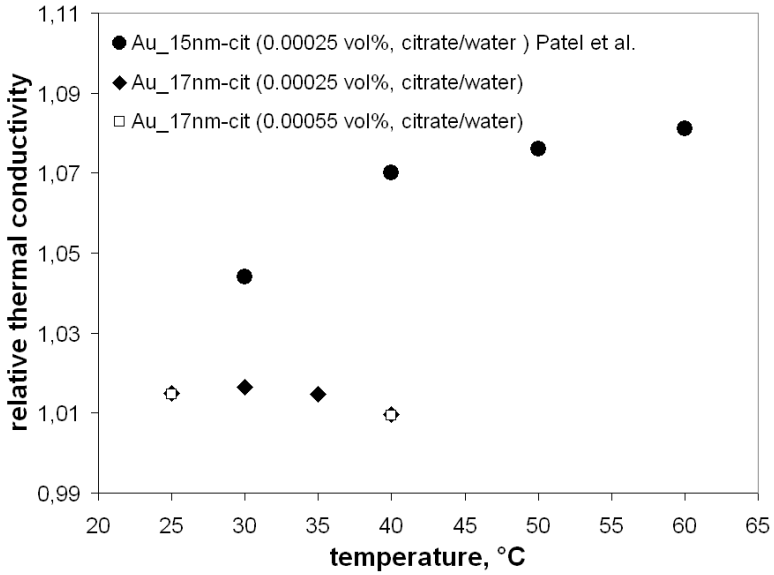

Figure 2.7. Relative thermal conductivity of gold-citrate nanofluids as a function of temperature.

Our experimental data at two volume fractions ($2.5\ 10^{-6}$ and $5.5\ 10^{-6}$) shows very similar behavior with quite small thermal conductivity enhancements and without any temperature dependence. Furthermore, we measured the thermal conductivity by means of both measurement techniques. The obtained data is in close agreement, whereby our results are additionally corroborated. Our observations deviate from the data of Patel et al.[3] where significant conductivity enhancement especially at elevated temperatures was reported. A possible reason for such an effect can be colloid destabilization causing particle clustering and/or their sedimentation on the detector surface and significantly change the thermal conductivity measurement in Patel et al.. In order to investigate possible destabilization of the colloid under heating we have performed light scattering measurement of naked colloids at different temperatures.

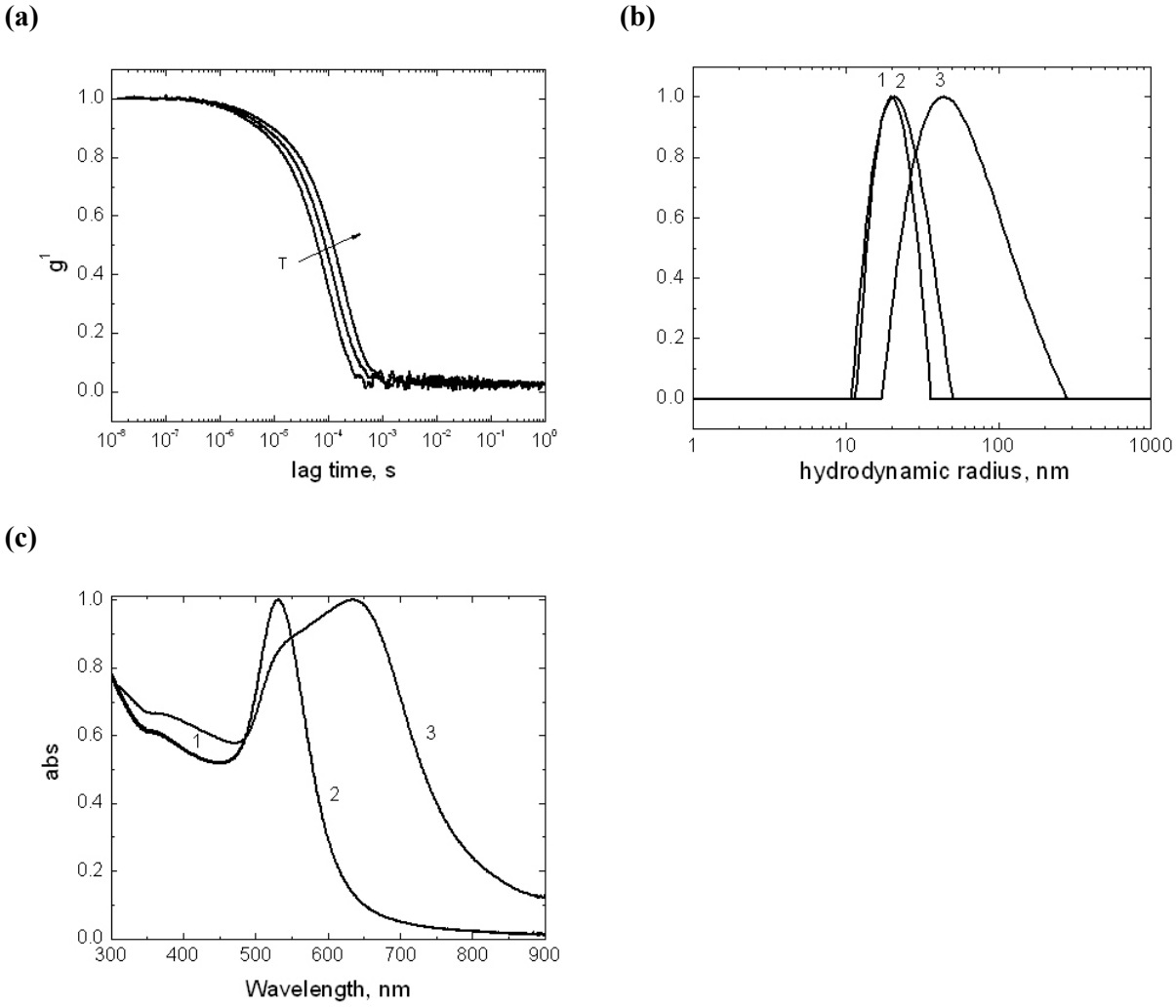

Figure 2.8. (a) The normalized electric field autocorrelation functions of 17 nm gold colloids at 0.55 mM at different temperatures: 20 ˚C, 40 ˚C and 60 ˚C. (b) particle size distributions of 40 nm gold colloids at 0.12 mM with different stabilizers: citrate (1), EGMUDE after reverse precipitation (2) and EGMUDE after simple citrate replacement (3). (c) UV-vis normalized spectra of 40 nm gold colloids at 0.12 mM with different stabilizers: citrate (1), EGMUDE after reverse precipitation (2) and EGMUDE after simple citrate replacement (3).

Figure 2.8a shows the correlation functions for the Au_17nm-citrate colloids at different temperatures. All correlation curves have the same shape and differ only in lag times. This shift results from decreasing water viscosity and therefore increasing diffusion coefficient of the gold nanoparticles. For all three curves the cumulative analysis provides a hydrodynamic radius of the particles of around 10 nm. Hence, we cannot observe any temperature dependency of the colloid clustering behavior.

Absence of any structural change of the nanofluid with 17 nm gold particles is well coherent with our invariant relative thermal conductivity at different temperature.

We also tested the influence of cluster formation on the thermal conductivity. Figure 2.8b shows particle size distributions of gold colloids of Au_40nm protected by different stabilizers at 0.12 mM. Citrate capped gold nanoparticles show quite low polydispersity with a mean hydrodynamic radius of 20 nm. After reverse precipitation[22] with EGMUDE protection the mean hydrodynamic radius grew up by 2.5 nm due to the additional layer of stabilizer. The polydispersity is almost the same, contrary to the behavior of particles after classical ligand exchange. There we observe not only much higher polydispersity but also increased mean hydrodynamic radius, which clearly implies relatively small (2-3 particles) clusters even in a well diluted colloid (at 0.12 mM). Those transformations were also confirmed by UV-vis spectroscopy (Fig 2.8c). The suspensions with citrate capped particles and stabilized by EGMUDE by means of reverse stabilization have almost the same spectra with small red-shift of 3 nm for Au-EGMUDE particles. On the other hand the UV-visible spectra of nanoparticles covered with EGMUDE by classical ligand exchange consists of a single particle plasmon band at 531 nm and a secondary surface plasmon band at 635 nm which is associated with formation of aggregates. The position of the latter depends on the interparticle separation (ligand length). According to Sendroiu et al.[31] the spectral aggregation shift becomes more pronounced with decreasing relative distance d/2R, where d is separation between particle centers and R is particle radius. For Au_40 nm-EGMUDE colloid prepared by classical ligand exchange the spectral aggregation shift is 635nm-531nm=104nm that corresponds to $d/2R \leq 1.1$ (see Sendroiu et al[31]). This means that the interfacial particle distance is much lower than 4 nm (20nm*2*1.1 - 20nm*2 = 4nm) that is less than double the length of EGMUDE molecule in an elongated state (2*2.76nm = 5.52nm). This can be related to incomplete citrate substitution by EGMUDE causing the cluster formation. Nevertheless, we do not observe any significant variations of the thermal conductivity for the samples with different particles stability.

Within the context of effective medium theory the largest possible increase of thermal conductivity for nanofluids with spherical particles at volume fraction $\varphi << 1$

will be $3\varphi\lambda_0$ (where λ_0 is thermal conductivity of basefluid) resulting in thermal conductivity enhancements < 1.8% for volume fractions $\varphi < 0.01$. Hence, all our data is consistent with effective medium theory.

2.5 Conclusions

In this paper, we produced stable gold colloids for a wide range of particle sizes (2 - 45 nm) and concentrations (0.00025 - 1 vol%). The particles are either protected solely by citrate ions or covered by chemically bounded ionic or nonionic stabilizers. We investigated the influence of these parameters as well as the temperature on the thermal conductivity of gold nanofluids by both GAP and THW methods. In spite of the large number of samples at different concentrations we did not observe a significant enhancement in thermal conductivity for any gold nanofluid. We additionally considered the effect of the particle clustering and did not find any dependence at least for small cluster sizes. The largest relative thermal conductivity of 1.014 was observed for the 0.11 vol% Au_40nm-EGMUDE nanofluid, whereas a similar enhancement was achieved for the Au_17nm-citrate nanofluid at a low gold concentration of 0.00055 vol%. Consequently we conclude that there is no abnormal thermal conductivity enhancement i.e. any deviation from classical effective medium theory for low concentrated well dispersed aqueous gold nanofluids.

Acknowledgement

We thank Andrey Shalkevich for his help with the DLS experiment and fruitful discussions. This work was supported by the Bundesamt fur Berufsbildung und Technologie in the frame of a KTI project.

2.6 References

1. Putnam, S. A.; Cahill, D. G.; Braun, P. V.; Ge, Z.; Shimmin, R. G., Thermal conductivity of nanoparticle suspensions. *Journal of Applied Physics* **2006,** 99, (8), 084308.
2. Liu, M.-S. L., Mark Ching-Cheng; Tsai, C.Y. ; Wang, C.-C., Enhancement of thermal conductivity with Cu for nanofluids using chemical reduction method. *International Journal of Heat and Mass Transfer* **2006,** 49, (17-18).
3. Patel, H. E.; Das, S. K.; Sundararajan, T.; Nair, A. S.; George, B.; Pradeep, T., Thermal conductivities of naked and monolayer protected metal nanoparticle based nanofluids: Manifestation of anomalous enhancement and chemical effects. *Applied Physics Letters* **2003,** 83, (14), 2931-2933.
4. Escher, W.; Michel, B.; Poulikakos, D., A Novel High Performance, Ultra Thin Heat Sink for Electronics. *International Journal of Heat and Mass Transfer* **2009,** Under Review.
5. Escher, W.; Michel, B.; Poulikakos, D., Efficiency of optimized bifurcating tree-like and parallel microchannel networks in the cooling of electronics. *International Journal of Heat and Mass Transfer* **2009,** 52, (5-6), 1421-1430.
6. Tuckerman, D. B.; Pease, R. F. W., IIIB-8 implications of high performance heat sinking for electron devices. *Electron Devices, IEEE Transactions on Electron Devices* **1981,** 28, (10), 1230-1231.
7. Hong, T.-K.; Yang, H.-S.; Choi, C. J., Study of the enhanced thermal conductivity of Fe nanofluids. *Journal of Applied Physics* **2005,** 97, (6), 064311-4.
8. Assael, M.; Metaxa, I.; Kakosimos, K.; Constantinou, D., Thermal Conductivity of Nanofluids – Experimental and Theoretical. *International Journal of Thermophysics* **2006,** 27, (4), 999-1017.
9. Li, C. H.; Peterson, G. P., Experimental investigation of temperature and volume fraction variations on the effective thermal conductivity of nanoparticle suspensions (nanofluids). *Journal of Applied Physics* **2006,** 99, (8), 084314.

10. Hwang, Y. J.; Ahn, Y. C.; Shin, H. S.; Lee, C. G.; Kim, G. T.; Park, H. S.; Lee, J. K., Investigation on characteristics of thermal conductivity enhancement of nanofluids *Current Applied Physics* **2006,** 6, (6), 1068.
11. Zhu, H. T.; Zhang, C. Y.; Tang, Y. M.; Wang, J. X., Novel Synthesis and Thermal Conductivity of CuO Nanofluid. *The Journal of Physical Chemistry C* **2007,** 111, (4), 1646-1650.
12. Lee, D., Thermophysical Properties of Interfacial Layer in Nanofluids. *Langmuir* **2007,** 23, (11), 6011-6018.
13. Choi, S. U. S.; Zhang, Z. G.; Yu, W.; Lockwood, F. E.; Grulke, E. A., Anomalous thermal conductivity enhancement in nanotube suspensions. *Applied Physics Letters* **2001,** 79, (14), 2252-2254.
14. Kang, H. U.; Kim, S. H.; Oh, J. M., Estimation of Thermal Conductivity of Nanofluid Using Experimental Effective Particle Volume. *Experimental Heat Transfer* **2006,** 19, (3), 181 - 191.
15. Brust, M.; Fink, J.; Bethell, D.; Schiffrin, D. J.; Kiely, C., Synthesis and reactions of functionalised gold nanoparticles. *Journal of the Chemical Society, Chemical Communications* **1995**, 1655.
16. Negishi, Y.; Takasugi, Y.; Sato, S.; Yao, H.; Kimura, K.; Tsukuda, T., Kinetic Stabilization of Growing Gold Clusters by Passivation with Thiolates. *The Journal of Physical Chemistry B* **2006,** 110, (25), 12218-12221.
17. Corbierre, M. K.; Lennox, R. B., Preparation of Thiol-Capped Gold Nanoparticles by Chemical Reduction of Soluble Au(I)−Thiolates. *Chemistry of Materials* **2005,** 17, (23), 5691-5696.
18. Negishi, Y.; Takasugi, Y.; Sato, S.; Yao, H.; Kimura, K.; Tsukuda, T., Magic-Numbered Aun Clusters Protected by Glutathione Monolayers (n = 18, 21, 25, 28, 32, 39): Isolation and Spectroscopic Characterization. *Journal of the American Chemical Society* **2004,** 126, (21), 6518-6519.
19. Gautier, C.; Burgi, T., Vibrational circular dichroism of N-acetyl-l-cysteine protected gold nanoparticles. *Chem Commun (Camb)* **2005**, (43), 5393-5.
20. Frens, G., Controlled nucleation for the regulation of the particle size in monodisperse gold suspensions. *Nature, Physical Science* **1973,** 241, (105), 20-22.

21. Enustun, B. V.; Turkevich, J., Coagulation of Colloidal Gold. *Journal of the American Chemical Society* **1963,** 85, (21), 3317-3328.
22. Shalkevich, N.; Shalkevich, A.; Si-Ahmed, L.; Bürgi, T., Reversible formation of gold nanoparticle - surfactant composite assemblies for the preparation of concentrated colloidal solutions. . In 2009.
23. Assael, M. J.; Karagiannidis, L.; Malamataris, N.; Wakeham, W. A., The Transient Hot-Wire Technique: A Numerical Approach. *International Journal of Thermophysics* **1998,** 19, (2), 379-389.
24. Assael, M. J.; Chen, C. F.; Metaxa, I.; Wakeham, W. A., Thermal Conductivity of Suspensions of Carbon Nanotubes in Water. *International Journal of Thermophysics* **2004,** 25, (4), 971-985.
25. Assael, M. J.; Charitidou, E.; Georgiadis, G. P.; Wakeham, W. A., Absolute measurement of the thermal conductivity of electrically conducting liquids. *Berichte der Bunsengesellschaft für Physikalische Chemie* **1988,** 92, (5), 627-631.
26. Lide, D. R., *CRC Handbook of Chemistry and Physics*. 89 ed.; 2008.
27. Barnett, R. N.; Cleveland, C. L.; Häkkinen, H.; Luedtke, W. D.; Yannouleas, C.; Landman, U., Structures and spectra of gold nanoclusters and quantum dot molecules. *The European Physical Journal D - Atomic, Molecular, Optical and Plasma Physics* **1999,** 9, (1), 95-104.
28. Schaaff, T. G.; Shafigullin, M. N.; Khoury, J. T.; Vezmar, I.; Whetten, R. L.; Cullen, W. G.; First, P. N.; Gutierrez-Wing, C.; Ascensio, J.; Jose-Yacaman, M. J., Isolation of Smaller Nanocrystal Au Molecules: Robust Quantum Effects in Optical Spectra. *The Journal of Physical Chemistry B* **1997,** 101, (40), 7885-7891.
29. Xie, H.; Wang, J.; Xi, T.; Liu, Y.; Ai, F.; Wu, Q., Thermal conductivity enhancement of suspensions containing nanosized alumina particles. *Journal of Applied Physics* **2002,** 91, (7), 4568-4572.
30. Hu, M.; Wang, X.; Hartland, G. V.; Salgueiriño-Maceira, V.; Liz-Marzán, L. M., Heat dissipation in gold–silica core-shell nanoparticles *Chemical Physics Letters* **2003,** 372, (5-6).

31. Sendroiu, I. E.; Mertens, S. F.; Schiffrin, D. J., Plasmon interactions between gold nanoparticles in aqueous solution with controlled spatial separation. *Phys Chem Chem Phys* **2006,** 8, (12), 1430-6.

Chapter 3

Thermal conductivity of aqueous suspensions of different ceramic nanomaterials

Thermal conductivity of aqueous suspensions of different ceramic nanomaterials

3.1 Abstract

Fluids with dispersed solid nanoparticles called nanofluids have great potential to improve the heat transfer behavior of conventional fluids. Different kind of commercial ceramic nanoparticles (AlN, Al_2O_3, $MgO*Al_2O_3$, ZnO, CuO, TiO_2, SiO_2, $SiO_2*Al_2O_3$) dispersed in water were investigated. Thermal conductivity of nanofluids was measured by transient hot wire technique. The effects of particle volume fraction, particle shape and dispersal agent were investigated. The results show that the thermal conductivity of the suspension depends on the thermal conductivities of both particles and the base fluid. The highest thermal conductivity increase of 31% was determined for AlN nanoparticle aqueous suspension with volume fraction of 7.2 % at 20 °C. The Hamilton-Crosser model was applied in order to estimate the thermal conductivity of ceramics suspensions and compared with experimental data.

3.2 Introduction

Cooling is one of the most essential challenges facing numerous industrial sectors including microelectronics, transportation, energy supply and production. Particularly, the developments of microelectronic devices with increased speeds (in the multi-GHz range) and smaller features (to <100 nm) require the advances in cooling include faster. The effective means for increasing heat dissipation is to enlarge the area that is available for heat exchange with a heat transfer fluid. Addition of nanoparticles in a fluid with poor heat transfer properties can greatly improve the latter. Pioneer works of Choi[1], Eastman[2], Masuda[3] and Lee[4] introduced the thermal conductivity enhancement of nanofluids to the science community. Nanofluids have higher thermal conductivity and aggregation stability, do not produce abrasion and

clogging in small passages and induce much smaller pressure drop in comparison with fluids containing particles of milli- or micrometer dimensions. A large number of experimental and theoretical studies of nanofluids with different kinds of dispersed solid phases have been reported. Research has shown that relatively small loading of nanoparticles, of the order of 5 volume per cent or less, can increase thermal conductivity of the base fluid to a large extent[5, 6]. Furthermore, the measured thermal conductivity of nanofluids is sometimes about one order of magnitude higher than that predicted by existing models based on effective medium theory. The latter is based on the three aspects such as spherical solid particles, their loading in the suspension and the thermal conductivities of the two components (solid and liquid). The classical model does not account for particle size, particle movement, particles interactions as well as for the effect of liquid layering on particle surface, which could influence on heat transfer through additional mechanism[7-15].

In our previous work[16] we prepared gold nanofluids and studied their capacity for thermal conductivity enhancement of the base fluid. In spite of the large thermal conductivity of bulk gold (316 W/(m*K)) and high volume fraction of gold nanoparticles in water (up to 1 vol%!) the stable gold colloids with various particle size and stabilizer layer did not exhibit any significant enhancement of thermal conductivity as it was reported earlier in the paper of Patel et al.[17]. They found thermal conductivity enhancement by up to 23.8 % at vanishing gold concentration of 0.00026 vol%. Such a large effect contradicts effective medium theory which predicts for a two-component (solid-in-liquid) mixture a maximum possible increase of thermal conductivity of $3\varphi\lambda_0$, where φ is the volume fraction of the dispersed solid phase and λ_0 is the thermal conductivity of the liquid medium). This would result in a thermal conductivity enhancement of 1.8% at a particle volume fraction of 0.01. The challenge in preparing stable gold colloids more concentrated than 1 vol% with relatively large nanoparticles can be attributed to some properties of gold itself. Heavy gold particles (density of 19.3 g/ml) in water with low viscosity have bigger tendency to agglomerate and precipitate than more lightweight and/or smaller particles due to larger kinetic energy and gravity. Therefore we explored the potential of less dense and much less expensive ceramic nanomaterials, which are widely used in various engineering applications.

The goal of this work is the preparation of aqueous suspensions of different commercial ceramics nanomaterials, the study of their thermal properties and comparison of experimental thermal conductivity with the one predicted by effective medium theory. The thermal conductivity measurements were carried out by KD2 Pro apparatus, which is based on the transient hot wire method.

3.3 Experimental part

3.3.1 Materials

AlN (100 nm), Al_2O_3 (50 nm), CuO (50 nm), ZnO (100 nm), TiO_2 (50 nm) nanopowders and 10 wt% $Ca_5(OH)(PO_4)_3$ (200nm), 34 wt% and 50 wt% SiO_2 (20 nm), 20 wt% SiO_2 alumina doped (50nm) aqueous suspensions were purchased from Sigma-Aldrich. TiO_2 (10nm*40 nm), $MgO*Al_2O_3$ (30 nm) nanopowders and 20 wt% Al_2O_3 (30 nm), 15 wt% TiO_2 (5-30 nm) and 40 wt% TiO_2 (30-50nm) aqueous suspensions were purchased from Nanostructured and Amorphous Materials Inc. Dispersal agents BYK- 154 (solution of an ammonium salt of an acrylate polymer) and CTAB (cetyltrimethylammonium bromide) were received from BYK Chimie and from Sigma-Aldrich respectively. Phosphoric acid H_3PO_4 (83-85%) was purchased from Reactolab SA and ethanol (99.9%) was obtained from Merck. All materials were used as received. Milli-Q water with a resistivity of 18.2 MΩ was employed.

3.3.2 Preparation of suspensions using commercial nanopowders

The nanopowder is immersed in stirred Milli-Q water or in solution of a suitable dispersant. The suspension with dispersant is stirred only slightly to avoid foam formation. After 5 minutes of stirring the suspension is ultrasonicated during 30 min.

Unprotected AlN powder undergoes a hydrolysis process when in contact with water. It transforms into γ-AlOOH, $Al(OH)_3$ or γ-Al_2O_3[18] according to the following reactions:

$$AlN_{(s)} + 2H_2O_{(l)} \rightarrow AlOOH_{(amorph)} + NH_{3\,(g)} \qquad [3.1]$$

$$AlOOH_{(amorph)} + H_2O_{(l)} \rightarrow Al(OH)_{3\,(gel)} \qquad [3.2]$$

$$NH_{3\,(g)} + H_2O_{(l)} \rightarrow NH_4^+{}_{(aq)} + OH^-{}_{(aq)} \qquad [3.3]$$

During the hydrolysis the surface of the powder is altered with undesirable aluminium hydroxides being formed which then transforms to bayerite ($Al(OH)_3$). The basic conditions produced promote flocculation of the powder and eventually gelling of the bayerite.

By passivating the surface of the AlN powder using small quantities of phosphoric acid, H_3PO_4, it is possible to protect the powder from water and avoid hydrolysis. This is thought to occur through the formation and adsorption of differing types of phosphate species at the surface of the particles, thus forming a protective layer.

We have used a modified method described by S. Fukumoto et al.[19] to protect the surface of 800 nm AlN particles. Briefly, 7.05 g of AlN powder was introduced in 27.8 ml of H_3PO_4 aq with pH 2.5 and stirred overnight. Then BYK-154 dispersant was added to the solution of AlN pre-treated with H_3PO_4 to enhance the solubility and the dispersion of latter due to the additional charge and steric stabilization by a bilayer of dispersant on the particle surface. The final colloid was agitated several hours and sonicated.

In the case of smaller AlN particles (100 nm) which are more susceptible to hydrolysis we have employed modified a nonaqueous processing[20]. For this, 45 ml of 10 wt% H_3PO_4 in ethanol was slowly added to 9.8 g of AlN powder suspended in 45 ml of ethanol and the mixture was stirred overnight. The treated AlN was filtered off and washed with ethanol to remove the excess of H_3PO_4 and then washed several times with water. The required quantity of BYK was added to the AlN suspension in water, agitated and then sonicated during 30 min.

3.3.3 Thermal conductivity measurement

We have used the KD2 Pro Analyzer to measure the thermal properties of nanoparticle suspensions. This device functions on the same principle as the transient hot wire technique which is described elsewhere[16]. The metal wire-sensor being immersed into sample is exposed to a step voltage resulting in a constant heat

generation along the wire. The transient rise in the wire temperature depends on the thermal conductivity of the surrounding sample whereas the sensor temperature is typically measured by the change of electrical resistance.

The commercial suspensions were tested as received. The suspensions prepared from the commercial nanopowders were sonicated during 30 min before thermal conductivity measurement. The temperatures of the sensor and the tested suspension were equilibrated and kept in the range from 20 °C to 22 °C.

3.4 Results and discussions

Experimental data for thermal conductivity of ceramic nanoparticles suspended in water are summarized in Table 3.1 and presented in Figure 3.1.

Table 3. 1. Summary of experimental thermal conductivities of aqueous suspensions of different ceramic nanomaterials and theoretically calculated thermal conductivities determined according to the Hamilton-Crosser model.

Particle material (size)	Thermal conductivity of particle (in bulk), W/(m*K)	Particle volume fraction, %	Dispersant (concentration)	Max. relative thermal conductivity Experimental data	Calculated relative thermal conductivity*
AlN	285				
<100 nm		5	BYK (0.1 vol%)	1.14	1.156
		10	BYK (0.2 vol%)	1.26	1.33
<800 nm		7.2		1.21 (15 min)	1.23
			BYK (0.1 vol%)	1.31 (15min)	
			BYK (0.1 vol%)	1.084 (120min)	
Al_2O_3	33.1				
30 nm		4		1.077	1.115
50 nm		5		1.11	1.149
$MgO*Al_2O_3$	24				
30 nm		7		1.072	1.208
		7	BYK	1.093	

			(0.1 vol%)		
SiO_2 20 nm	1.38	 9 15.5 22.7		 1.029 1.08 1.16	 1.083 1.145 1.218
SiO_2*Al_2O_3 <50 nm	1.76	 6.2		 1.056	 1.066
TiO_2 <50 nm 10x40 nm 5-30 nm 30-50 nm	11.7	 5 1 2 5 1 5 3.8 9.5	 CTAB (0.05 wt%) CTAB (0.05 wt%)	 1.12 1.013 1.027 1.093 1.02 1.131 0.938 0.639	 1.135 1.046 1.092 1.235 1.046 1.235 1.101 1.266
ZnO <100 nm	110	 3		 1.11	 1.091
CuO <50 nm	20	 1 2 3		 0.96 0.84 0.79	 1.027 1.056 1.084
$Ca_5(OH)(PO_4)_3$ <200 nm		 4		 1.025	

*Thermal conductivity of water (base fluid) is taken 0.6062 W/(m*K) at 25 °C**.**

In Figure 3.1 two groups of samples can be distinguished. One of them (most of the tested suspensions) shows an increased thermal conductivity with respect to the base fluid and a direct dependence of thermal conductivity on the thermal conductivity of solid nanoparticles and their loading in the base fluid. Another group demonstrates decreased thermal conductivity relative to the base fluid, which gets more pronounced with increasing particle volume fraction. The latter effect can be attributed to a large content of surfactant (and/or additional solvents in commercial products). Surfactant is utilized to improve the solubility of the nanopowder and/or the aggregative stability of the suspension. The much lower thermal conductivity of the surfactant compared to water can diminish the thermal conductivity of the suspension.

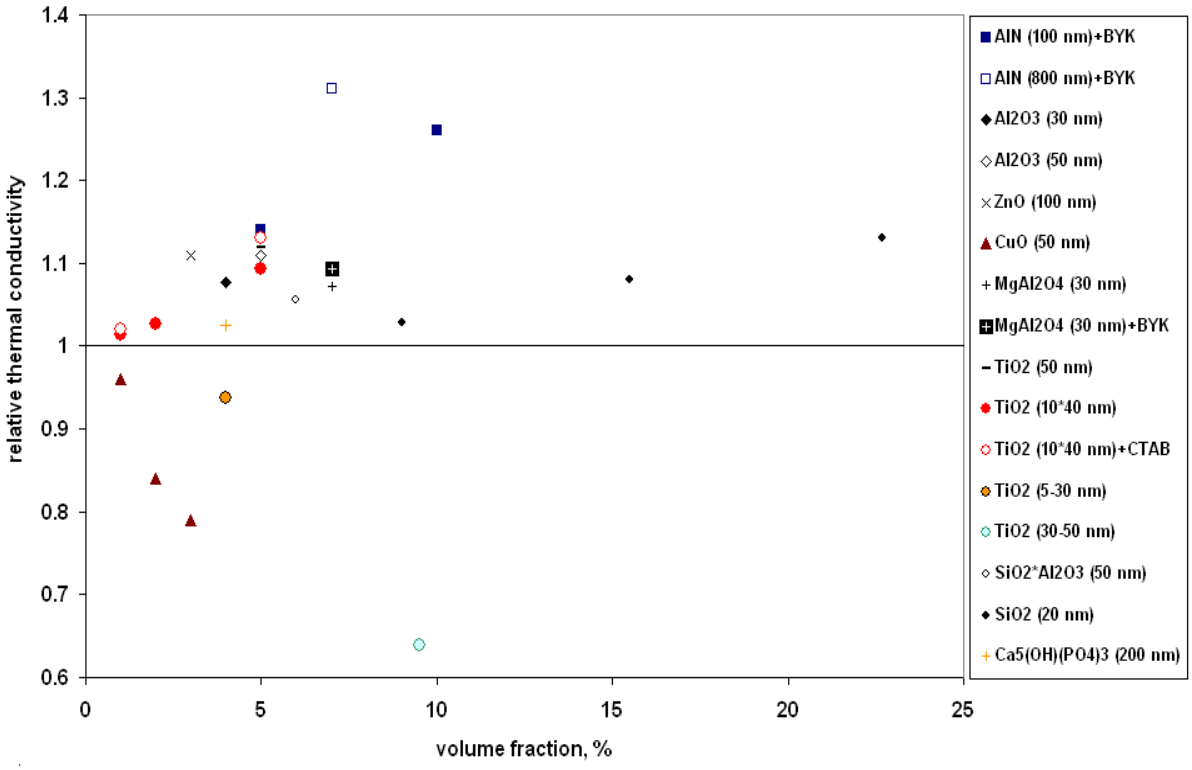

Figure 3. 1. Relative thermal conductivity of ceramic nanosuspensions as a function of particle volume fraction.

The thermal conductivity of colloids can be enhanced through addition of a small amount of surfactant that results in increased aggregative stability of the colloids and hence much slower particle sedimentation. It therefore provides the permanent "effective" concentration of particles in solution that affects the thermal conductivity values. The influence of surfactant on thermal conductivity can be seen in Figures 3.2 and 3.3. The effect of a dispersant becomes more pronounced with increasing of particle volume fraction (Figure 3.2). Thus, the suspension of TiO_2_10*40nm stabilized with CTAB shows larger thermal conductivity enhancement of 4 % at 5 vol% than at 1 vol% (0.7 % enhancement) in comparison with the suspension at the same particle concentrations without any surfactant. This shows the increased importance of stabilization by a surfactant at higher volume fraction. The thermal conductivities of concentrated (7 vol%), additionally stabilized

suspensions of $MgO*Al_2O_3$_30 nm (Figure 3.2) and AlN_800nm (Figure 3.3) are 2% and 10% higher than the thermal conductivities of these suspensions without surfactant. In this case i.e. for highly concentrated colloids the effect of thermal conductivity of the solid dispersed phase on thermal conductivity of the suspension becomes more prominent.

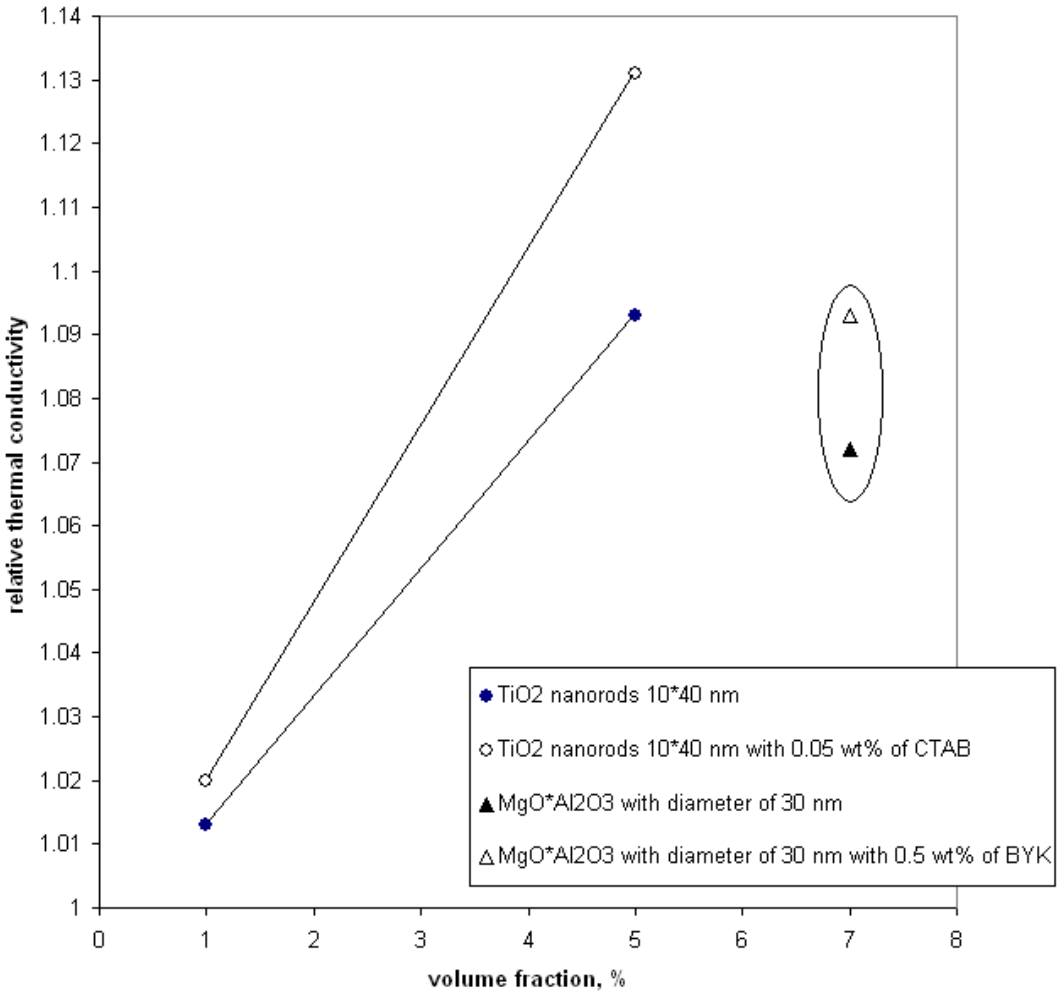

Figure 3. 2. Thermal conductivity of the TiO_2_10*40nm (o) and $MgO*Al_2O_3$_30nm (Δ) suspensions without any dispersal agent (filled symbols) and after an addition of surfactant (open symbols).

In Figure 3.3 we can see how a small amount of surfactant changes the thermal conductivity of suspension as a function of time. All suspensions with a small amount of surfactant have enlarged values of thermal conductivity. Thus, 5 vol% suspension of 10*40nm TiO_2 particles stabilized by CTAB and 10 vol% suspension of 100 nm AlN particles covered by BYK exhibit stable thermal conductivities during several hours whereas the same non stabilized suspensions show considerable thermal conductivity drop during the first 30 minutes. The AlN suspension with the largest particles of 800 nm that we have studied in this work exhibits the highest thermal conductivity, which is however time-dependent. The thermal conductivity of the AlN_800nm suspension with BYK or without dispersal agent greatly decreases as some settling is taking place. The AlN particles of 100 nm stabilized by BYK demonstrate invariable 26% enhancement of thermal conductivity for several hours due to the better steric and charge protection of the smaller particles with the same surfactant.

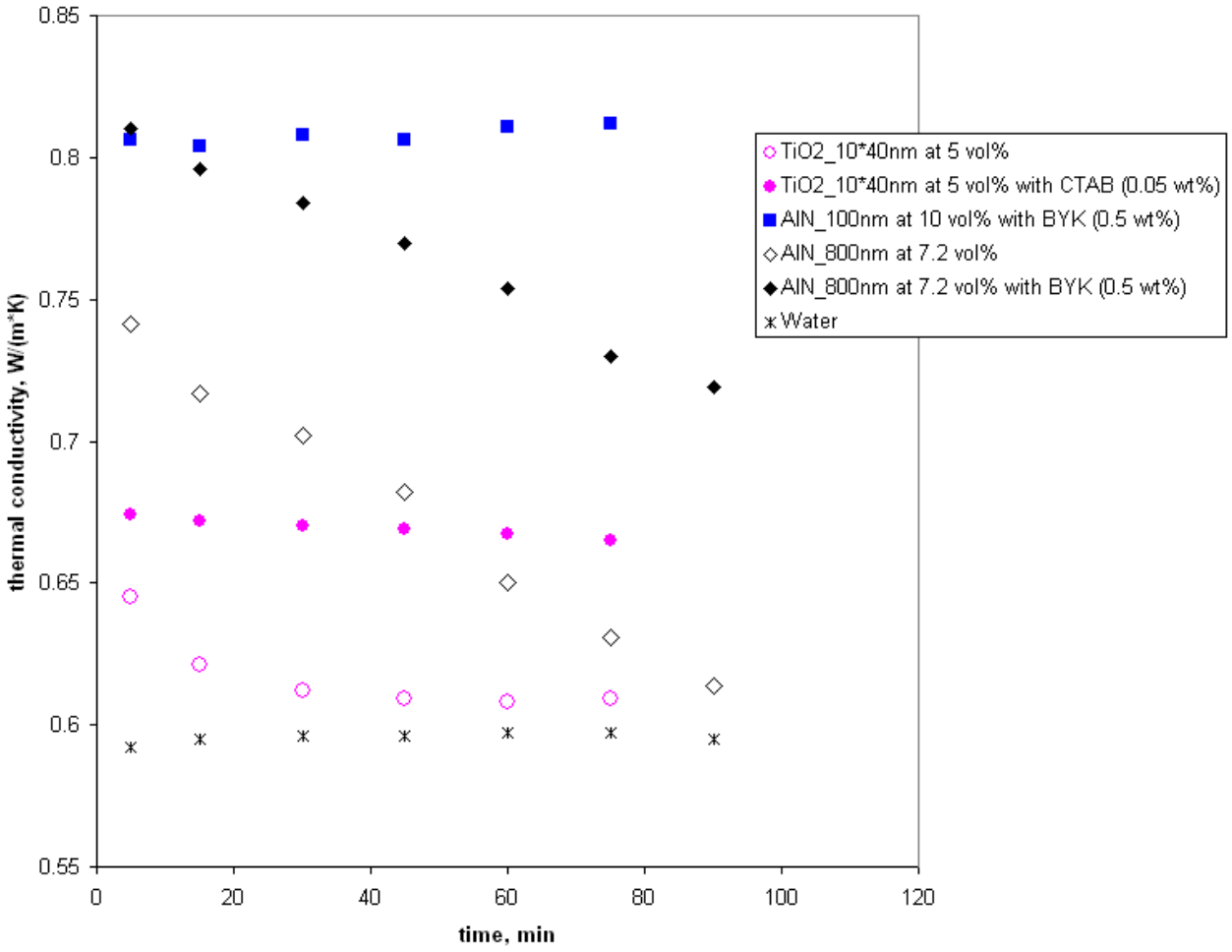

Figure 3. 3. Effect of a dispersal agent on the thermal conductivity of AlN and TiO_2 suspensions as a function of time.

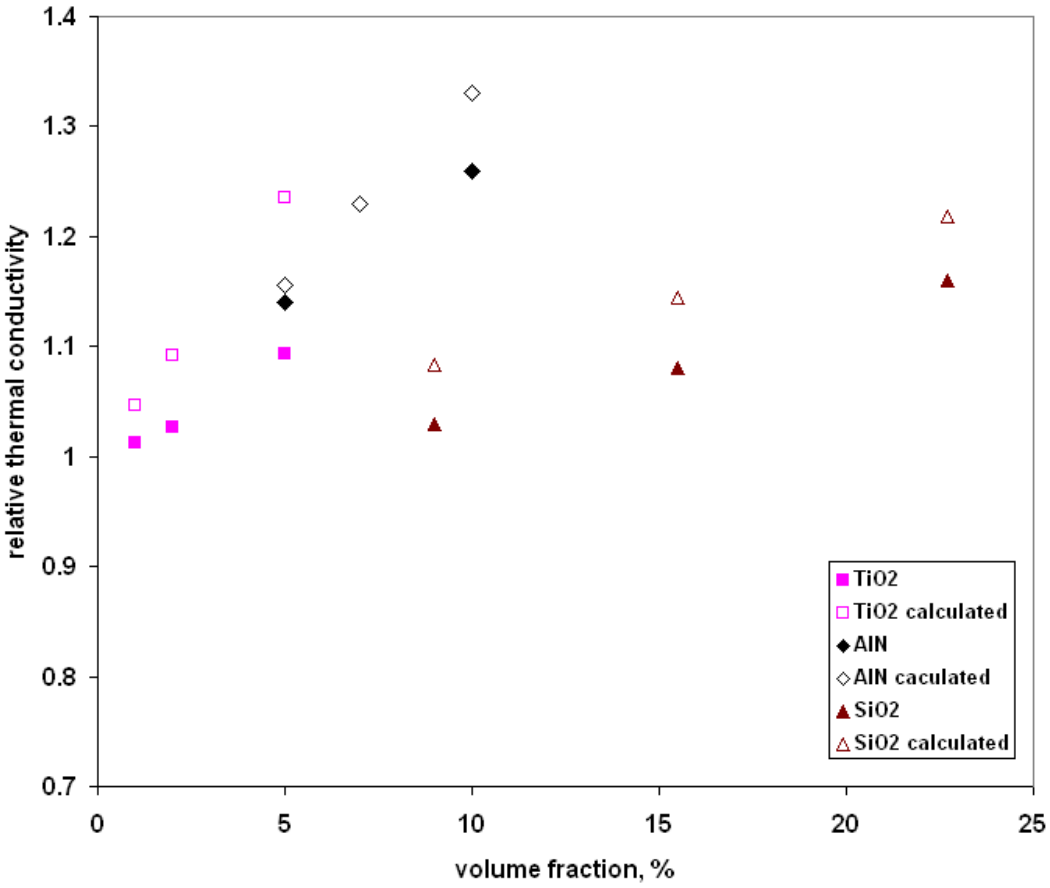

Figure 3. 4. Relative thermal conductivity as a function of the particle volume fraction. Experimental data for TiO_2_10*40nm (□), AlN_100nm (◊) and SiO_2_20nm (Δ) aqueous suspensions (filled symbols) and relative thermal conductivity predicted by Hamilton-Crosser model (open symbols).

In Figure 3.4 we compare experimental and theoretical data of thermal conductivity of AlN, TiO_2 and SiO_2 suspensions at different particle loading. There are various theories developed to calculate the thermal conductivity of solid particle suspensions. Most of them are based on the Maxwell-Garnett model for two-component solid-liquid mixtures which uses conductivity of phase constituents and volume fractions and assumes stationary nanoparticles in the continuous medium, and is therefore called a static model. In the present investigation the Hamilton-Crosser model was employed because it takes into account an effect of particle shape, particle volume fraction and thermal conductivities of the two components of a suspension i.e. the dispersed solid phase and the liquid medium of the dispersion. The Hamilton-Crosser model is given in the next form

$$\frac{\lambda_e}{\lambda_0} = \frac{\lambda_p + (n-1)\lambda_0 - (n-1)(\lambda_0 - \lambda_p)\varphi}{\lambda_p + (n-1)\lambda_0 + (\lambda_0 - \lambda_p)\varphi} \qquad [3.4]$$

where λ_e = effective thermal conductivity of suspension/ W m^{-1} K^{-1}

λ_0 = thermal conductivity of dispersion liquid medium / W m^{-1} K^{-1}

λ_p = thermal conductivity of dispersed solid phase / W m^{-1} K^{-1}

φ = volume fraction of dispersed solid phase

n = shape factor which equals 3 or 6 for spheres or for cylinders, respectively

The comparison of experimental and theoretical data shows the difference between measured and calculated thermal conductivity values. The thermal conductivity in the both cases is almost linearly dependent on the particle concentration but the experimental values are mainly lower than predicted by the model. Only the experimentally determined thermal conductivity of ZnO suspension was larger than calculated (see Table 3.1). Also, we could not establish a shape-dependence of thermal conductivity of the tested suspensions according to the model predictions. We obtained discrepancies between the Hamilton-Crosser model and experimental data for TiO_2 suspensions with spherical and rod-like particles at 5 vol% (see Table 3.1). The nanorods enhance the thermal conductivity of the base fluid but their contribution in heat transfer is lower than in the case of nanospheres. The disagreement in calculated and measured data could be related, on the one hand, to some difficulties in preparation of concentrated suspensions from nanopowders (low homogenization of particles in water, difficult removal of air bubbles from highly viscous suspension etc.) and, on the other hand, to insufficient information about composition of the commercial nanomaterials. Moreover, the used theoretical model predicts the thermal conductivity of two-component colloids but it does not consider factors such as particle size, particle interaction, the liquid layering on the particle surface, liquid convection etc. which could contribute to heat transfer. Addionally, an examination of the phonon theory for the thermal conductivity of ceramics[21, 22] indicates that the boundary scattering that occurs due to the size of the nanoparticles is lower than for the bulk material. This effect, if factored into the Maxwell model,

would result in an even lower effective thermal conductivity of nanopasrticle suspensions.[23]

It is difficult to identify an established model for the prediction of thermal conductivity of colloids. Particle and liquid movement, particle-liquid and particle-particle interactions should play key roles for the heat transfer performance of colloids. Therefore, in the next chapter we will try to clarify the role of the two factors particle motion and particle interactions in heat transfer for silica and alumina colloids.

3.5 Conclusions

Aqueous suspensions with different kind of ceramics nanomaterials have been prepared. The thermal conductivity of these suspensions has been measured by a transient hot wire technique. The experimental results show a linear dependence of thermal conductivity on particle volume fraction. The highest thermal conductivity increase of 31% was found for an AlN suspension at 7.2 vol%. We have also observed an effect of dispersal agent. Small amount of surfactant increases aggregative stability of tested suspensions and enhances their thermal conductivity. The experimental data and theoretically calculated data on thermal conductivity of ceramic nanoparticle suspensions have been summarized and discussed. The Hamilton-Crosser model has been used to estimate the thermal conductivity of the suspensions.

3.6 References

1. Choi, U. S., Enhancing thermal conductivity of fluid with nanoparticles. In *Developments and Applications of Non-Newtonian Flows, ASME FED-231.*, P., S. D. A. a. W. H., Ed. New York, 1995; pp 99-105.
2. Eastman, J. A.; Choi, U. S.; Li, S.; Thompson, L. J.; Lee, S. In *Enhanced thermal conductivitythrough the development of nanofluids.*, Materials Research Society Symposium, Pittsburgh, 1997; Materials Research Society: Pittsburgh, 1997; pp 3-11.
3. Masuda, H.; Ebata, A.; Teramae, K.; Hishinuma, N., Alteration of thermal conductivity and viscosity of liquid by dispersing ultra-fine particles (dispersion of Al2O3, SiO2, and TiO2 ultrafine particles. *Netsu Bussei* **1990,** 4, 227-233.
4. Lee, S.; Choi, S. U.-S.; Li, S.; Eastman, J. A., Measuring Thermal Conductivity of Fluids Containing Oxide Nanoparticles. *Journal of Heat Transfer* **1999,** 121, (2), 280-289.
5. Eastman, J. A.; Choi, S. U. S.; Li, S.; Yu, W.; Thompson, L. J., Anomalously increased effective thermal conductivities of ethylene glycol-based nanofluids containing copper nanoparticles. *Applied Physics Letters* **2001,** 78, (6), 718-720.
6. Choi, S. U. S.; Zhang, Z. G.; Yu, W.; Lockwood, F. E.; Grulke, E. A., Anomalous thermal conductivity enhancement in nanotube suspensions. *Applied Physics Letters* **2001,** 79, (14), 2252-2254.
7. Jang, S. P.; Choi, S. U. S., Role of Brownian motion in the enhanced thermal conductivity of nanofluids. *Applied Physics Letters* **2004,** 84, (21), 4316-4318.
8. Kang, H. U.; Kim, S. H.; Oh, J. M., Estimation of Thermal Conductivity of Nanofluid Using Experimental Effective Particle Volume. *Experimental Heat Transfer* **2006,** 19, (3), 181 - 191.
9. Keblinski, P.; Phillpot, S.; Choi, S.; Eastman, J., Mechanisms of heat flow in suspensions of nano-sized particles (nanofluids). *International Journal of Heat and Mass Transfer* **2002,** 45, 855-863.

10. Evans, W.; Fish, J.; Keblinski, P., Role of Brownian motion hydrodynamics on nanofluid thermal conductivity. *Applied Physics Letters* **2006,** 88, (9), 093116.
11. Prasher, R.; Phelan, P. E.; Bhattacharya, P., Effect of Aggregation Kinetics on the Thermal Conductivity of Nanoscale Colloidal Solutions (Nanofluid). *Nano Letters* **2006,** 6, (7), 1529-1534.
12. Eapen, J.; Li, C.; Yip, S., Mechanism of Thermal Transport in Dilute Nanocolloids. *Physical Review Letters* **2007,** 98, (2), 028302.
13. Prasher, R.; Song, D.; Wang, J.; Phelan, P., Measurements of nanofluid viscosity and its implications for thermal applications. *Applied Physics Letters* **2006,** 89, (13), 133108.
14. Xue, L.; Keblinski, P.; Phillpot, S. R.; Choi, S. U.-S.; EASTMAN, J. A., Effect of liquid layering at the liquid-solid interface on thermal transport. *International journal of heat and mass transfer* **2004,** 47, (19-20), 4277-4284.
15. Yu, C. J.; Richter, A. G.; Kmetko, J.; Dugan, S. W.; Datta, A.; Dutta, P., Structure of interfacial liquids: X-ray scattering studies. *Physical Review E* **2001,** 63, (2), 021205.
16. Shalkevich, N.; Escher, W.; Bürgi, T.; Michel, B.; Si-Ahmed, L.; Poulikakos, D., A study on the thermal conductivity of gold nanoparticle colloids. *Langmuir, accepted for publication* **2009**.
17. Patel, H. E.; Das, S. K.; Sundararajan, T.; Nair, A. S.; George, B.; Pradeep, T., Thermal conductivities of naked and monolayer protected metal nanoparticle based nanofluids: Manifestation of anomalous enhancement and chemical effects. *Applied Physics Letters* **2003,** 83, (14), 2931-2933.
18. Nicolaescu, I. V.; Tardos, G.; Riman, R. E., Thermogravimetric determination of carbon, nitrogen and oxygen in aluminum nitride. *Journal of American Ceramic Society* **1994,** 77, (9), 2265-72.
19. Fukumoto, S.; Hookabe, T.; Tsubakino, H., Hydrolysis behavior of aluminum nitride in various solutions. *Journal of Materials Science* **2000,** 35, (11), 2743-2748.
20. Ganesh, I.; Olhero, S. M.; Araujo, A. B.; Correia, M. R.; Sundararajan, G.; Ferreira, J. M. F., Chemisorption of Phosphoric Acid and Surface

Characterization of As Passivated AlN Powder Against Hydrolysis. *Langmuir* **2008,** 24, (10), 5359-5365.

21. Berman, R., *Thermal conduction in solids* Oxford [Eng.] : Clarendon Press: 1976; p 61.
22. Klemens, P. G., In *Thermal Conductivity*, Gaal, P., Ed. Destech: Lancaster, 2005; Vol. 28, pp 304-317.
23. Li, C. H.; Peterson, G. P., Experimental investigation of temperature and volume fraction variations on the effective thermal conductivity of nanoparticle suspensions (nanofluids). *Journal of Applied Physics* **2006,** 99, (8), 084314.

Chapter 4

Thermal conductivity of concentrated colloids in different states

Thermal conductivity of concentrated colloids in different states

Authors: Natallia Shalkevich, Andrey Shalkevich and Thomas Bürgi

4.1 Abstract

The thermal conductivity of concentrated colloids in fluid, glass and gel states was analyzed. SiO_2 colloids at 10-31 vol% and Al_2O_3 colloids at 4.8 vol% in the fluid, the gel and the glassy states were studied with dynamic light scattering, rheology and transmission electron microscope. Thermal conductivity of the three states was measured as a function of volume fraction. For the fluid and gel states the thermal conductivity increases almost linearly with concentration, reaching roughly 18 % enhancement at silica volume fraction of 31 vol%. In contrast, in the glass state thermal conductivity strongly decreases with increasing volume fraction.

Keywords: Thermal conductivity, silica, alumina, glass, gel, nanofluid, dynamic light scattering

4.2 Introduction

Heat transfer is very important in many industrial and technical processes. Various fluids are commonly used as heat conductors. Nevertheless, they have too low thermal conductivity for certain applications and various additives are used in order to improve the situation. The most common way is the addition of dispersed solid particles to the fluid. The thermal conductivity of the suspension with milli- or micrometer-sized well-dispersed particles can be estimated within effective medium theory by the classical Maxwell-Garnett model[1-3]. This model is based on different aspects such as the spherical solid particle, volume fraction and thermal conductivity of fluid and solid materials and generally works for a low thermal conductivity ratio (~10) between the solid and the fluid. The Maxwell-Garnett model was further extended by several investigators who included the effect of shape[4, 5], particle interactions[2, 6-11], and particle distribution[12]. Meanwhile there are many experimental data which have shown that composite fluid with nanoparticles, also known as nanofluids, have much higher thermal conductivity as predicted by effective medium theory[13].

A number of publications[2, 14-16] on thermal properties of nanofluids show very large enhancements in the thermal conductivity of nanofluids. The most extreme results were obtained for different allotropes of carbon. For example, enormous enhancements of thermal conductivity by 160% and by 70% were observed for a suspension containing 1% of MWCNTs in oil[16] and for 1% ultra-dispersed diamond in ethylene glycol respectively[2]. Currently, there are several routes for explaining the mechanism responsible for unusually high thermal transport properties of nanofluids, such as effects of the liquid layering at solid interface[17-19], the particle Brownian motion[20-23] and the particle clustering[2, 6-11].

One of the major mechanisms of thermal conductivity enhancement is the layering of the solvent molecules on the particle surface. Liquid molecules form an ordered solid-like layer around the particle that would have a thermal conductivity higher than the bulk liquid medium (Keblinski et al.[17, 24]) and could give a path for

rapid heat transfer between a solid particle and the base fluid. Liquid layering theory was shown to be promising but it uses as adjustable parameter the thickness of the liquid layer. Furthermore, experimental verification is not trivial at all.

Brownian motion of nanoparticles can influence the thermal conductivity by two independent scenarios. The first of them[20, 21] assumes that the particles with higher kinetic energy absorb the heat from the fluid surrounding them, migrate to new region and there release the thermal energy to surrounding liquid thereby enhancing the thermal transport. But Evans et al. have recently demonstrated[25] that such a contribution of Brownian motion of nanoparticles to heat transfer is negligible in comparison with much faster thermal diffusion through the base fluid. A second scenario[23] is based on the hydrodynamic effect of the moving particles which results in locally ordered microconvections of base fluid around each nanoparticle. Recent molecular dynamics simulations made by Evans et al[26] revealed that the hydrodynamic Brownian motion mechanism has only a minor effect on the effective thermal conductivity for a relatively high particle volume fraction (ca 3.3 vol%).

Depending on the chemistry of the system aggregation of particles can take place. At constant volume fraction the probability of aggregation increases with decreasing particle size, because the average interparticle distance decreases, making the attractive Van der Waals force more important.[22] Large and sparse clusters can even decrease thermal conductivity[8] while chain-like clusters pass through the whole volume and significantly enhance heat transfer[6], which was recently confirmed by simulations[7, 8, 27]. Keblinski and Prasher write that the thermal conductivity enhancement is mainly attributed to the ability of the heat to move rapidly along the backbone of the aggregate named also as a high-conductivity percolation path. Some experimental observations confirmed the role of the clustering in the increase of thermal conductivity of nanofluids.[8-10] John Philip et al.[10] demonstrated 216% enhancement of thermal conductivity for magnetite nanofluid in applied magnetic field (101 Gauss) where Fe_3O_4 nanoparticles form chain-like structure.

The present work investigates the effect of the particles motion and arrangement on the thermal conductivity of colloidal suspensions. We are going to compare thermal properties of a system of freely moving particles (fluid) with suspensions

where particles are “frozen” i.e. restricted in translational motion (gel and glass). Moreover we are going to test an influence of the particle-particle contact on the heat transfer by comparison of a system with interconnected particles (gel) and one with fully separated particles (glass). For this purpose, we used two kinds of nanoparticles with significantly different thermal conductivity in the solid state. Scattering methods as well as rheology were applied to determine their degree of motion and to observe the overall structure of these suspensions.

4.3 Experimental section

4.3.1 Materials

Ludox-grade TMA and TM colloidal silica (22 nm in diameter) suspensions in deionized water (34 wt% for TMA and 50 wt% for TM) were purchased from Aldrich-Sigma. Colloidal alumina (30 nm in diameter) suspension in water (20 wt%) was purchased from Nanostructured and Amorphous Materials Inc. All reagents were used as received. Dowex DM80 was purchased from Aldrich-Sigma. Milli-Q (Millipore) water with a resistivity of 18.2 MΩ was employed throughout.

4.3.2 Instrumentation

The rheological behavior of dispersions was studied with a MCR 300 rheometer (Paar Physica) in temperature-controlled narrow-gap Mooney-Ewart geometry.[28] All tests were done at 25 ^{o}C.

Dynamic light scattering (DLS) was performed with an ALV-5000 spectrophotometer equipped with an argon-laser (Coherent, model Innova 300, λ = 488 nm), a digital autocorrelator (ALV) and variable angle detection system. Measurements were made at a fixed scattering angle of 90° and a temperature of 25.0 ± 0.1 $^{\circ}$C. The individual correlation functions were analyzed using a second-order cumulant fit. Gel and glass samples were studied with DLS measurements by using 3D cross correlation setup from LS Instruments GmbH, Fribourg, Switzerland. This instrument allows the suppression of multiple scattering as described in detail elsewhere.[29]

Transmission electron micrographs (TEM) were obtained with a Philips C 200 microscope in bright field mode at a voltage of 200 kV. The samples for TEM study were prepared by casting a few drops of the colloid onto carbon-coated copper grids (300 mesh) and used after solvent evaporation in air.

The KD2 Themal Properties Analyzer from Decagon was used for all measurement of the thermal conductivity and it works on a similar principle to the transient hot wire method. It calculates the thermal conductivity of samples by

measuring the dissipation of energy from a line heat source[30]. Each measurement takes a total of ninety seconds, leaving the temperature to stabilize during the first thirty, heating for the second thirty and determining the rate of cooling in the final thirty seconds with final values of thermal conductivity being quoted to an accuracy of 5%. The KD2 works on the assumption that the probe is an infinitely long heat source and that the solution being measured is homogeneous, isotropic and of a uniform initial temperature. Of course, these assumptions are only true to a certain extent and introduce varying degrees of error in the final value but for the purposes of these measurements can be supposed to be correct. The relationship between ΔT and ln(t) can be shown as in [30]:

$$T - T_0 \cong \frac{q}{4\pi\lambda_h}\left(\ln(t) - \gamma - \ln\left(\frac{r^2}{4\kappa}\right)\right)$$

where T = temperature / K

T_0 = initial temperature / K

q = heat produced per unit length per unit time / W m^{-1}

λ_h = thermal conductivity of the medium / W m^{-1} C^{-1}

t = time / s

γ = Euler's to determinate their degree of motion constant

r = radial distance / m

κ = thermal diffusivity / m^2 s^{-1}

By plotting ΔT against ln(t) the thermal conductivity is then simply calculated from the gradient of the slope, m, which is equal to $\left(\frac{q}{4\pi\lambda_h}\right)$.

4.3.3 Preparation of colloids

4.3.3.1 Formation of gel state

One of the common routes of gel formation is a collapse of the electrical double layer (EDL) on the particle surface by adding of electrolyte. Obviously, the Coulomb repulsion is now so strongly screened that interparticle van der Waals attractions become dominant and the particles become unstable. Destabilized particles stick together and form a percolated network. Macroscopic properties of gel are determined by the network parameters (density, bond strength etc.) which depend on the composition and the concentration of added electrolyte[31]. Sodium (or potassium) chloride is normally used as destabilizing agent to prepare a gelled colloid. At concentration of 0.2 M this salt can reduce the EDL thickness down to 1 nm[31] and stabilizing repulsion forces become negligible.

The colloids of SiO_2 (Al_2O_3) nanoparticles in water were prepared as follows. Several drops of 7-8 M solution of NaCl were added in 50 ml of silica (alumina) aqueous suspension up to 0.2 M final concentration of NaCl. This suspension was stirred 5 minutes and kept for several days to equilibrate and form the network structure. Samples for the dynamic light scattering were prepared directly in the measuring cell in order to avoid structure distortion.

4.3.3.2 Formation of glass state

To prepare a colloid in glassy state we have to increase the EDL of particles which can be realized by adding of exchange resin. The latter removes the counterions from the colloid thus increasing the electrical double layer. Extending the EDL, the interparticle electrostatic repulsion forces and effective volume of EDL-particle increase simultaneously. Once the moving of the particles becomes restricted at finite threshold and the cage effect is observed when the particles motion is limited in space bound to neighbor-particles. In this case the particles are well separated one from another i.e. there is no direct contact between particles. The absence of particle translational motion eliminates the solvent convection. Furthermore the majority of the solvent molecules are immobilized in the EDL and therefore traditional heat transfer due to the diffusion of solvent is significantly reduced.

In order to form the glassy state an initial nanoparticle colloid of required concentration was mixed with ion exchange resin (Dowex) in quantity of 1/5 from total volume. The mixture was kept at least for 1 week to remove excess of ions. Once the resin was mixed with the suspension we periodically (2 times per day) agitated the sample tube. Afterwards the thickened dispersion was filtered through 5-μm pore size Millipore filters to remove all ion-exchanged beads.

4.4 Results

We have studied suspensions of silica and alumina nanoparticles with diameters of 22 nm and 30 nm, respectively. Their sizes were confirmed by transmission electron microscopy (TEM) imaging as shown in Figure 4.1.

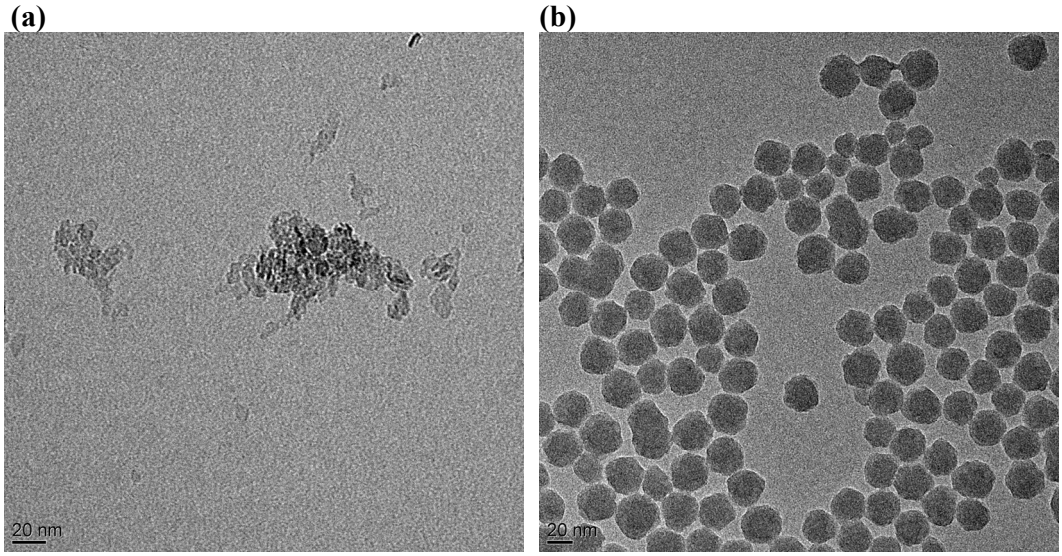

Figure 4. 1. Transmission electron microscopy graphs of alumina (a) and silica (b) nanoparticles.

While silica particles have spherical shape and diameter of 22 nm as reported by the producer the alumina particles are irregularly shaped with considerable polydispersity (10-30 nm) and probably porous morphology. In order to connect those observations with the structure in the fluid samples we performed DLS measurement on the most diluted samples and a subsequent cumulant fit of the correlation

functions. The silica suspension exhibits low polydispersity and mean hydrodynamic radius of 16 nm in the concentration range from 0.2 to 19 vol% (Figure 4.2a). The increase of diameter of small silica particles determined by DLS as compared to TEM is well known and normally attributed to the roughness and/or hairing of the silica surface[32, 33]. Alumina suspension demonstrates distinctly different behaviour. Dynamic light scattering does not only reveal the signal from individual (and rather polydisperse) particles but indicates the existence of very polydisperse clusters with mean hydrodynamic radius of around 100 nm (Figure 4.2b).

(a) **(b)**

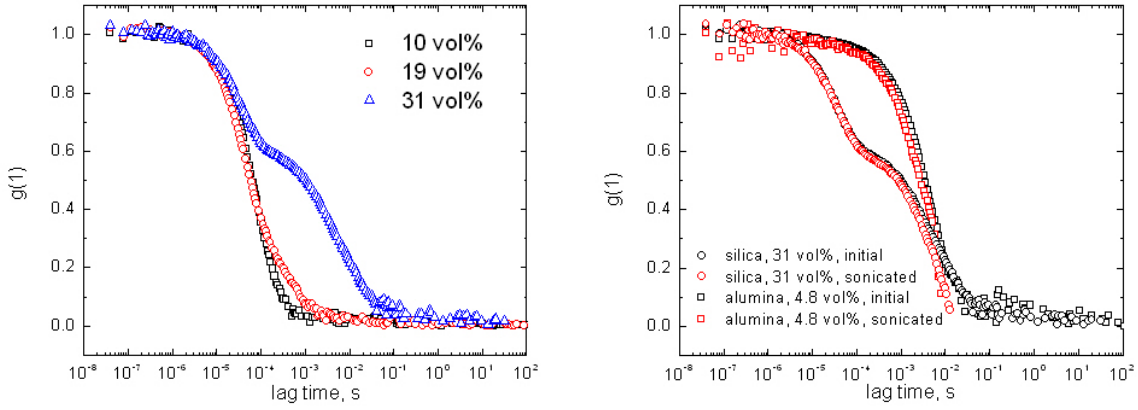

Figure 4. 2. Measured intensity correlation functions as a function of decay time for (a) silica suspensions at different concentrations and (b) a silica and alumina suspension in initial states and after sonication.

The influence of the cluster formation on the thermal conductivity of nanofluids has been reported in many studies. Therefore, we have tested the effect of particles concentration on the presence of particle clusters (aggregates) and the results for three concentrations of silica are shown in Figure 4.2a. While samples with 10 and 19 vol% of silica have almost the same behavior and no aggregates the suspension with maximum silica concentration demonstrates clear sign of aggregates. To test the stability of the clusters we have performed dynamic light scattering measurements of initial suspensions and after treatment with a Branson sonifier 250 over 15 minutes at

the setting duty-cycle 50%, output control 5. A shown in Figure 4.2b both the silica and alumina suspensions do not exhibit significant change after ultrasonic treatment either due to high stability of aggregates or their fast reassembly due to the high concentration of the particles. Nevertheless, a small amount of clusters (which are intermediate state between individual particles and gel network) in the fluid is expected to have a much smaller influence on the thermal conductivity of the fluid than a fully established percolated network.

To test macroscopic structures of different colloid states and their influence on the heat transfer we performed rheological measurements of silica suspensions at 19 vol%. We have used the same batch of initial silica nanoparticle suspension (TMA) for the preparation of all colloidal states at the same concentration and therefore only the difference is particle interactions and structure. Results are shown in Figure 4.3.

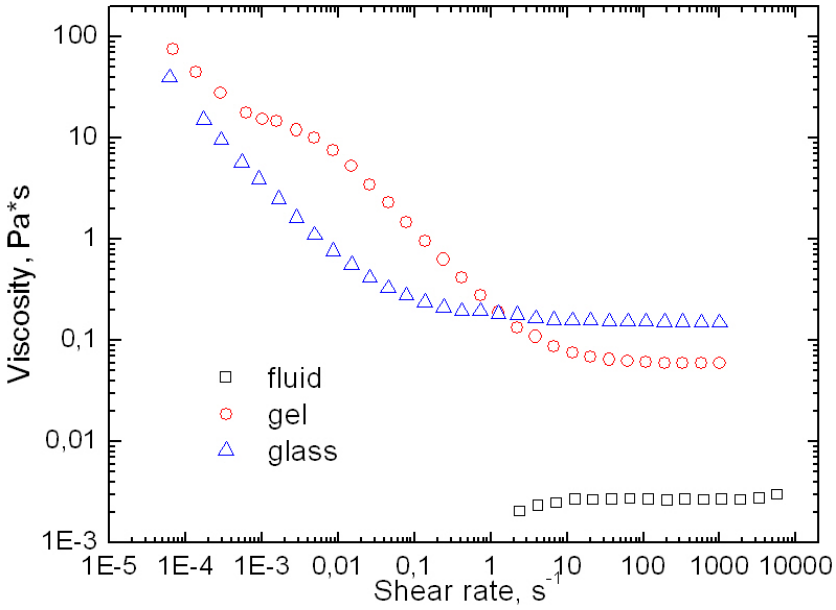

Figure 4. 3. Viscosity as a function of shear rate for silica suspensions of 19 vol% in fluid, gel and glass state.

Fluid-like sample exhibits typical behavior of Newtonian fluid with viscosity independent on the shear rate. Due to low viscosity values we were able to detect significant shear stress only at high shear rates. Upon decreasing shear rates the viscosity drops down and becomes undetectable. For structured colloidal dispersions

(gel and glass) subjected to steady shear we observed that we have a high-shear Newtonian plateau at accessible shear rates. At low shear values the glassy and gelled samples exhibit the shear-thinning behavior with slope of -1 over more than two decades in shear rates which is similar to the behavior observed previously in colloidal suspensions undergoing a liquid-solid transition[28]. A weak plateau for the gel-like sample at low shear rates can be the result of complex structural properties of the sample such as network subunits which require additional shear stress to break.

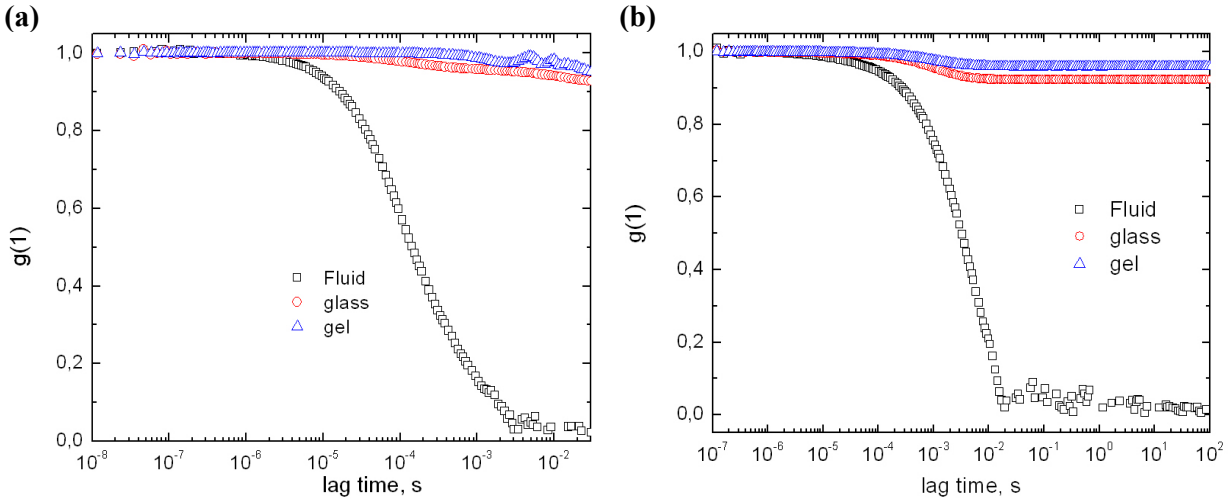

Figure 4. 4. Measured intensity correlation functions as a function of decay time for different states of (a) a 19 vol% silica suspension and (b) a 4.8 vol% alumina suspension.

In order to study the local dynamics of the particles in different colloidal states we have again performed dynamic light scattering. Results are presented in Figure 4.4. We observed almost the same behavior for the gel and glass states where we see clearly nonergodic behavior as a result of structure formation. While the fluid sample demonstrates classical Brownian motion of particles, the nonergodic samples have only traces of self diffusion and very slow collective diffusion motion. The both suspensions of silica and alumina particles exhibit the same peculiarities and indeed can be compared for the heat transfer.

Experimental data for the relative thermal conductivity of silica and alumina in different colloidal states are summarized in the Figure 4.5. MilliQ water was used as the reference base fluid for the fluid sample. For the gel and glass systems the water base fluid was additionally modified in order to gain accurate relative thermal conductivity values. We have used 0.2 M solution of sodium chloride for the gelled colloids and for glassy samples the water was treated with Dowex exchange resin. Thermal conductivity of the reference base fluid was measured independently at the same temperature as colloids. The temperature of measurement was kept at 22±1 °C.

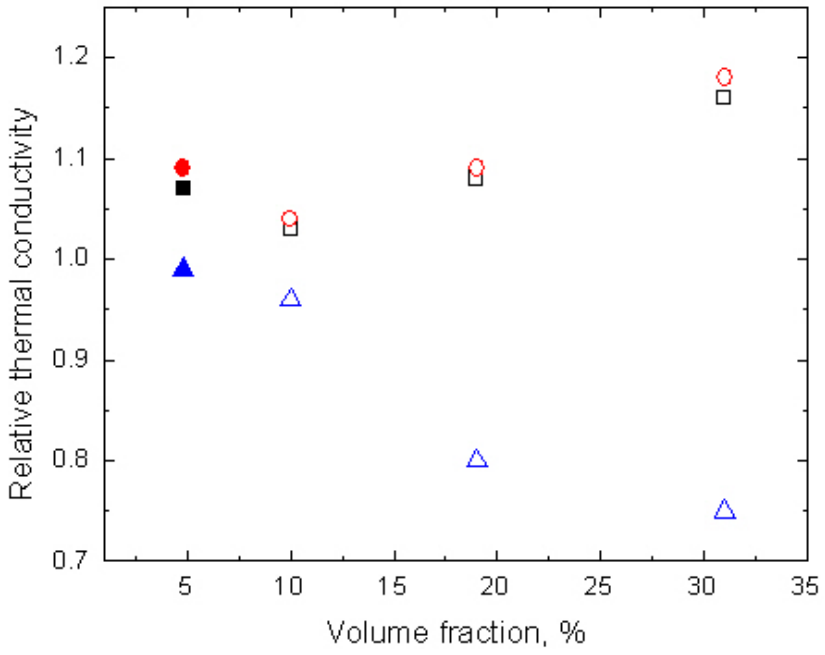

Figure 4. 5. Relative thermal conductivity of silica (open symbols) and alumina (filled symbols) supensions in fluid (□), gel (O) and glass (Δ) states as a function of concentration.

Thermal conductivity of silica suspensions in fluid and gel states increases almost linearly with concentration showing a maximum thermal conductivity of 0.706 $W \cdot K^{-1}m^{-1}$ or 18% enhancement for gel state at a volume fraction of 31%. Similar behavior of silica colloids in fluid state was observed by other groups[34]. In contrast, thermal conductivity of glass state strongly decreases with increasing volume fraction and drops down to 0.449 $W \cdot K^{-1}m^{-1}$ or -25% for the glass with silica concentration of

31 vol%. Alumina suspensions at lower volume fraction of 4.8 vol% demonstrate higher thermal conductivity enhancement than silica suspensions at 10 vol% in fluid and gel states as well as a larger improvement for the gelled sample. The glassy alumina sample does not exhibit any significant thermal conductivity enhancement.

4.5 Discussion

Main speculations on the enhanced thermal conductivity of nanofluids relate to Brownian motion[20, 21, 23] and to the nanoparticles organization in the fluid[6-9]. Thus, the Brownian motion of the particles is drastically changed if particles aggregate and form clusters and/or networks. Aggregation may influence as well the liquid layering effect due to decreasing of accessible particle surface for the solvent molecules. We have observed that the gelled samples which form networks of directly contact nanoparticles demonstrate slightly better thermal conductivity enhancement than the fluid state. This indicates that Brownian motion does not play the key role in heat transfer of concentrated suspensions. Direct interparticle contacts in the gelled sample are more important for heat transfer as can also be seen in the case of alumina nanoparticle suspensions.

We observe more pronounced thermal conductivity enhancement of 3% for fluid and gel alumina samples than for samples with silica particles. This could be attributed to much higher thermal conductivity of pure alumina (33.09 W/(m*K))[35] than pure silica (1.38 W/(m*K))[36].

In glass samples the particles are frozen in cages formed by neighboring particles due to highly expanded electrical double layer. Therefore we expected to see the influence of solvent layering at particles surfaces. Surprisingly we have detected significantly decreased heat transfer of the samples in comparison with water. That tendency could only be explained in terms of changing water properties, in our case immobilization of water molecules in electrical double layers of particles. Water molecules immobilized at surface strongly limited in motion and therefore retain lower kinetic energy. As soon as water shows strong decreasing of thermal conductivity with lowering temperature we expect that immobilized water have

similar tendency. This hypothesis is also supported by strong decreasing of the effect with lowering of particles volume fraction, i.e. amount of immobilized water molecules.

4.6 Conclusions

In order to understand the mechanism of heat transfer we have prepared different states of nanofluids based on the same nanoparticles, i.e. 22 nm SiO_2 and 30 nm Al_2O_3 particles, in aqueous suspension. We investigated the fluid, the gel and the glass state at equal volume fractions. Rheology was performed to show the behavior of different colloidal states on the macroscopic level. The gelled and glassy silica samples demonstrate a shear-thinning behavior whereas the silica fluid exhibits typical behavior of a Newtonian fluid with an average particle diameter of 22 nm. Dynamic light scattering was used to inspect the local dynamics of the particles in the glass, the gel and the fluid colloids. The silica and alumina samples in gel and glass states demonstrate almost the same behavior of nonergodic colloids as a result of structure formation. In contrast, the fluid samples demonstrate more or less classical Brownian motion of particles. The silica nanofluid is a monodisperse suspension with hydrodynamic particle radius of 16 nm. DLS study of alumina nanofluid reveals a polydisperse system with the clusters of about 100 nm.

Thermal conductivity of the three states was measured as a function of volume fraction. For the fluid and gel states thermal conductivity increases almost linearly with concentration. Both the silica and alumina colloids in the gel state exhibit the highest thermal conductivity enhancements i.e. 18% enhancement for SiO_2 at a volume fraction of 31 vol% and 10% enhancement for Al_2O_3 at 4.8 vol%. In contrary, in the glass state thermal conductivity strongly decreases with increasing volume fraction. The drastic difference in thermal conductivity enhancement of the glass (-25%) and the gel (+18 %) is rather surprising and requires deeper investigation.

4.7 References

1. Das, S. K.; Choi, S. U. S.; Patel, H. E., Heat Transfer in Nanofluids. *Heat Transfer Engineering* **2006,** 27, (10), 3 - 19.
2. Kang, H. U.; Kim, S. H.; Oh, J. M., Estimation of Thermal Conductivity of Nanofluid Using Experimental Effective Particle Volume. *Experimental Heat Transfer* **2006,** 19, (3), 181 - 191.
3. Maxwell, J. C., *Electricity and magnetizm*. Clarendon Press: Oxford, 1873.
4. Assael, M.; Metaxa, I.; Kakosimos, K.; Constantinou, D., Thermal Conductivity of Nanofluids – Experimental and Theoretical. *International Journal of Thermophysics* **2006,** 27, (4), 999-1017.
5. Hamilton, R.; Crosser, O. K., Thermal conductivity of heterogeneous two-component systems. *Industrial and Engineering Chemistry Fundamentals* **1962,** 1, (3), 187-191.
6. Eapen, J.; Li, J.; Yip, S., Beyond the Maxwell limit: Thermal conduction in nanofluids with percolating fluid structures. *Physical Review E (Statistical, Nonlinear, and Soft Matter Physics)* **2007,** 76, (6), 062501.
7. Prasher, R.; Evans, W.; Meakin, P.; Fish, J.; Phelan, P.; Keblinski, P., Effect of aggregation on thermal conduction in colloidal nanofluids. *Applied Physics Letters* **2006,** 89, (14), 143119.
8. Prasher, R.; Phelan, P. E.; Bhattacharya, P., Effect of Aggregation Kinetics on the Thermal Conductivity of Nanoscale Colloidal Solutions (Nanofluid). *Nano Letters* **2006,** 6, (7), 1529-1534.
9. Xuan, Y.; Li, Q.; Hu, W., Aggregation structure and thermal conductivity of nanofluids. *AIChE Journal* **2003,** 49, (4), 1038-1043.
10. Philip, J.; Shima, P. D.; Raj, B., Nanofluid with tunable thermal properties. *Applied Physics Letters* **2008,** 92, (4), 043108.
11. Wang, B.-X.; Zhou, L.-P.; Peng, X.-F., A fractal model for predicting the effective thermal conductivity of liquid with suspension of nanoparticles *International Journal of Heat and Mass Transfer* **2003,** 46, (14), 2665-2672.

12. Huaqing, X.; Jinchang, W.; Tonggeng, X.; Yan, L.; Fei, A.; Qingren, W., Thermal conductivity enhancement of suspensions containing nanosized alumina particles. *Journal of Applied Physics* **2002,** 91, (7), 4568-4572.
13. Hwang, Y. J.; Ahn, Y. C.; Shin, H. S.; Lee, C. G.; Kim, G. T.; Park, H. S.; Lee, J. K., Investigation on characteristics of thermal conductivity enhancement of nanofluids *Current Applied Physics* **2006,** 6, (6), 1068.
14. Krishnamurthy, S.; Bhattacharya, P.; Phelan, P. E.; Prasher, R. S., Enhanced Mass Transport in Nanofluids. *Nano Letters* **2006,** 6, (3), 419-423.
15. Eastman, J. A.; Choi, S. U. S.; Li, S.; Yu, W.; Thompson, L. J., Anomalously increased effective thermal conductivities of ethylene glycol-based nanofluids containing copper nanoparticles. *Applied Physics Letters* **2001,** 78, (6), 718-720.
16. Choi, S. U. S.; Zhang, Z. G.; Yu, W.; Lockwood, F. E.; Grulke, E. A., Anomalous thermal conductivity enhancement in nanotube suspensions. *Applied Physics Letters* **2001,** 79, (14), 2252-2254.
17. Keblinski, P.; Phillpot, S.; Choi, S.; Eastman, J., Mechanisms of heat flow in suspensions of nano-sized particles (nanofluids). *International Journal of Heat and Mass Transfer* **2002,** 45, 855-863.
18. Leong, K. C.; Yang, C.; Murshed, S. M. S., A model for the thermal conductivity of nanofluids – the effect of interfacial layer. *Journal of Nanoparticle Research* **2006,** 8, (2), 245-254.
19. Lee, D., Thermophysical Properties of Interfacial Layer in Nanofluids. *Langmuir* **2007,** 23, (11), 6011-6018.
20. Jang, S. P.; Choi, S. U. S., Role of Brownian motion in the enhanced thermal conductivity of nanofluids. *Applied Physics Letters* **2004,** 84, (21), 4316-4318.
21. Prasher, R.; Bhattacharya, P.; Phelan, P. E., Thermal conductivity of nanoscale colloidal solutions (nanofluids). *Phys Rev Lett* **2005,** 94, (2), 025901.
22. Gharagozloo, P. E.; Eaton, J. K.; Goodson, K. E., Diffusion, aggregation, and the thermal conductivity of nanofluids. *Applied Physics Letters* **2008,** 93, (10), 103110.

23. Peterson, G. P.; Li, C. H., Heat and Mass Transfer in Fluids with Nanoparticle Suspensions. In *Advances in Heat Transfer*, Harnett, J. P.; Irvine, T. F., Eds. Pergamon Press: New York, 2005; Vol. 39, pp 257-370.
24. Keblinski, P.; Thomin, J., Hydrodynamic field around a Brownian particle. *Phys Rev E Stat Nonlin Soft Matter Phys* **2006,** 73, (1 Pt 1), 010502.
25. Evans, W.; Fish, J.; Keblinski, P., Role of Brownian motion hydrodynamics on nanofluid thermal conductivity. *Applied Physics Letters* **2006,** 88, (9), 093116.
26. Evans, W.; Fish, J.; Keblinski, P., Thermal conductivity of ordered molecular water. *J Chem Phys* **2007,** 126, (15), 154504.
27. Patel, H. A.; Garde, S.; Keblinski, P., Thermal resistance of nanoscopic liquid-liquid interfaces: dependence on chemistry and molecular architecture. *Nano Lett* **2005,** 5, (11), 2225-31.
28. Shalkevich, A.; Stradner, A.; Bhat, S. K.; Muller, F.; Schurtenberger, P., Cluster, glass, and gel formation and viscoelastic phase separation in aqueous clay suspensions. *Langmuir* **2007,** 23, (7), 3570-80.
29. Urban, C.; Schurtenberger, P., Characterization of Turbid Colloidal Suspensions Using Light Scattering Techniques Combined with Cross-Correlation Methods. *Journal of Colloid and Interface Science* **1998,** 207, (1), 150.
30. KD2 Manual. In Decagon.
31. Hunter, R. J., *Foundations of Colloid Science*. Oxford University Press: New York, 2001.
32. Gittings, M. R.; Saville, D. A., The determination of hydrodynamic size and zeta potential from electrophoretic mobility and light scattering measurements. *Colloids and Surfaces A: Physicochemical and Engineering Aspects* **1998,** 141, (1), 111-117.
33. Kobayashi, M.; Skarba, M.; Galletto, P.; Cakara, D.; Borkovec, M., Effects of Heat Treatment on the Aggregation and Charging of Stöber-type Silica. *Journal of colloid and interface science* **2005,** 292, (1), 139-147.

34. Chen, G.; Yu, W.; Singh, D.; Cookson, D.; Routbort, J., Application of SAXS to the study of particle-size-dependent thermal conductivity in silica nanofluids. *Journal of Nanoparticle Research* **2008,** 10, (7), 1109-1114.

35. (Editor), D. R. L., *CRC Handbook of Chemistry and Physics*. 88 ed.; CRC: 2007.

36. Grove, A. S., *Physics and Technology of Semiconductor Devices*. John Wiley and Sons: 1971.

Conclusions

- We synthesized gold nanoparticles with various stabilizing agents in a wide range of particle sizes (2 - 45 nm) and we prepared stable gold nanocolloids in a wide range of particle loading (0.00025 - 1 vol%).
- We have developed a new method of preparation of stable concentrated (up to 0.1 vol%) gold nanocolloids via reversible nanoparticle-surfactant composite assemblies.
- Thermal conductivity of gold and of different ceramic nanofluids was studied as a function of particle size, volume fraction, stabilizer layer and temperature.
- We received moderate thermal conductivity enhancement for the studied nanofluids that is consistent with effective medium theory. The considerable thermal conductivities reported before for very diluted gold nanoparticles could not be confirmed.
- The thermal conductivity of concentrated silica and alumina nanocolloids in fluid, glass and gel states was analyzed for understanding the mechanism of heat transfer in nanocolloids. It was found that Brownian motion of particles does not play a key role in heat transfer in concentrated colloids whereas a direct interparticle contact is more important.

Appendix

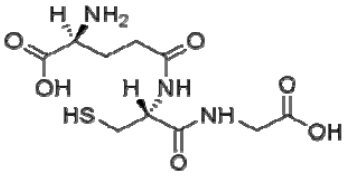

glutathione (GSH)

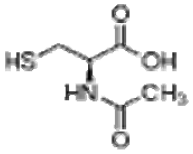

N-acetyl-L-cysteine (NAC)

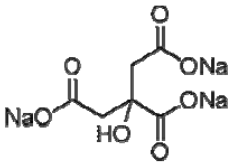

Trisodium citrate

triethyleneglycol-11-mercaptoundecylether (EGMUDE)

Acknowledgements

I would like to thank all people who helped and supported me during three years of my research and study at the University of Neuchâtel.

I am grateful to Prof. Thomas Bürgi who has given me the opportunity to conduct this work in his laboratory and was always been very understanding and open for discussions. His confidence in me had a great impact on my development as a scientist.

I thank Prof. Frank Scheffold, Prof. Helen Stöckli-Evans and Prof. Georg Süss-Fink agreeing to be co-examiners of my thesis.

I would like to express my acknowledgement to Prof. Helen Stöckli-Evans for her support and help during the last year of my thesis work.

Many thanks to all my colleagues from the Surface Spectroscopy and Nanoscience Laboratory: Julien Boudon, Igor Dolamic, Cyrille Gautier, Silvia Angeloni-Suter, Marco Bieri, Qiaoling Li, Alastair Cunningham and Satyabrata Si for their help in every day work and incredible atmosphere that they created by their sense of humor and kindness.

I would also like to thank all the members of NINCO project for the useful and stimulating discussions and successful collaboration.

I am grateful to Dr. Massoud Dadras and Mrs. Mireille Leboeuf for their help with introduction to the electron microscopy.

Great thanks to my family, relatives and all my friends for their understanding, support, love and friendship during this thesis work. Огромное спасибо вам, дорогие мои!

Curriculum vitae

Natallia Vladimirovna Shalkevich

Personal data

Nationality: Belarus
Date of birth: December 17, 1975
Civil status: married, two children

Education

September 2006 – present	PhD thesis with Prof. Dr. Thomas Bürgi Surface Spectroscopy and Nanosciences Laboratory Institute of Physics, University of Neuchâtel, Switzerland.
Sept. 1993 – Jul. 1998	Diploma in Chemistry, Diploma thesis in physical chemistry with Prof. A.I. Kulak Belarusian State University, Minsk, Belarus.
1983 - 1993	34th primary, secondary and high school in Minsk, Belarus

Publications

Natallia Shalkevich, Andrey Shalkevich and Thomas Bürgi, Thermal conductivity of concentrated colloids in different states. *Ready for submission*.

W. Escher, T. Brunschwiler, N. Shalkevich, T. Bürgi, B. Michel and D. Poulikakos, On the cooling of electronics with nanofluids. *Submitted to ASME Journal of Heat Transfer*.

Natallia Shalkevich, Andrey Shalkevich, Lynda Si-Ahmed and Thomas Bürgi, Reversible formation of gold nanoparticle surfactant composite assemblies for the preparation of concentrated colloidal solutions. *Physical Chemistry Chemical Physics* **2009**, in press, DOI: 10.1039/B912571J.

Natallia Shalkevich, Werner Escher, Thomas Bürgi, Bruno Michel, Lynda Si-Ahmed and Dimos Poulikakos, On the Thermal Conductivity of Gold Nanoparticle Colloids. *Langmuir* **2009**, Article ASAP, DOI: 10.1021/la9022757.

Igor Dolamic, Cyrille Gautier, Julien Boudon, Natallia Shalkevich and Thomas Bürgi, Adsorption of Thiol-Protected Gold Nanoparticles on TiO2 and Their Behavior under UV Light Irradiation. *Journal of Physical Chemistry C* **2008**, 112(15), 5816-5824.